1-1-2012

Integrated seat and suspension control for a quarter car with driver model

Haiping Du
University of Wollongong, hdu@uow.edu.au

Weihua Li
University of Wollongong, weihuali@uow.edu.au

Nong Zhang
University Of Technology Sydney

Integrated seat and suspension control for a quarter car with driver model

Abstract

In this paper, an integrated vehicle seat and sus pension control strategy for a quarter car with driver model is proposed to improve suspension performance on driver ride comfort. An integrated seat and suspension model that includes a quarter-car suspension, a seat suspension, and a 4-degree-of freedom (DOM) driver body model is presented first. This in1 tegrated model provides a platform to evaluate ride comfort 1performance in terms of driver head acceleration responses under typical road disturbances and to develop an integrated control of seat and car suspensions. Based on the integrated model, an H∞ state feedback controller is designed to minimize the driver head acceleration under road disturbances. Considering that state variables for a driver body model are not measurement available in practice, a static output feedback controller, which only uses measurable state variables, is designed. Further discussion on robust multiobjective controller design, which considers driver body parameter uncertainties, suspension stroke limitation, and road-holding properties, is also provided. Last, numerical simula tions are conducted to evaluate the effectiveness of the proposed control strategy. The results show that the integrated seat and sus pension control can effectively improve suspension ride comfort performance compared with the passive seat suspension, active seat suspension control, and active car suspension control.

Keywords

era2015, model, driver, car, quarter, control, integrated, suspension, seat

Disciplines

Engineering | Science and Technology Studies

Publication Details

Du, H., Li, W. & Zhang, N. (2012). Integrated seat and suspension control for a quarter car with driver model. IEEE Transactions on Vehicular Technology, 61 (9), 3893-3908.

Integrated seat and suspension control for a quarter-car with driver model

Haiping Du * **Weihua Li** † **Nong Zhang** ‡

May 18, 2012

Abstract

In this paper, an integrated vehicle seat and suspension control strategy for a quarter-car with driver model is proposed to improve suspension performance on driver ride comfort. An integrated seat and suspension model which includes a quarter-car suspension, a seat suspension, and a four degree-of-freedom (DOF) driver body model is presented at first. This integrated model provides a platform to evaluate ride comfort performance in terms of driver head acceleration responses under typical road disturbances and to develop an integrated control to seat and car suspensions. Based on the integrated model, a H_∞ state feedback controller is designed to minimise the driver head acceleration under road disturbances. Considering that state variables for driver body model are not measurement available in practice, a static output feedback controller, which only uses measurable state variables, is designed. Further discussion on robust multiobjective controller design

*School of Electrical, Computer and Telecommunications Engineering, University of Wollongong, Wollongong, NSW 2522, Australia. Email: hdu@uow.edu.au.

†School of Mechanical, Materials and Mechatronic Engineering, University of Wollongong, Wollongong, NSW 2522, Australia.

‡Mechatronics and Intelligent Systems, Faculty of Engineering, University of Technology, Sydney, P.O. Box 123, Broadway, NSW 2007, Australia.

which considers driver body parameter uncertainties, suspension stroke limitation and road holding property is also provided. At last, numerical simulations are conducted to evaluate the effectiveness of the proposed control strategy. The results show that the integrated seat and suspension control can effectively improve suspension ride comfort performance compared to the passive seat and suspension, active seat suspension control, and active car suspension control.

Keywords: vehicle suspension, seat suspension, driver body model, integrated control, static output feedback control

1 Introduction

Seat suspension has been commonly accepted in commercial vehicles for industrial, agricultural and other transport purposes [1] to provide driver ride comfort, to reduce driver fatigue due to long hour driving or exposure to severe working environment such as rough road condition, and to improve driver safety and health [2]. Study on optimisation and control of seat suspensions for reducing vertical vibration has been an active topic for decades. Three main types of seat suspensions, i.e., passive seat suspension, semi-active seat suspension, and active seat suspension, have been presented so far. The study on passive seat suspension mainly focuses on parameter optimisation for the spring stiffness and the damping coefficient. In general, small spring stiffness may get good ride comfort, however, it will incur a large suspension deflection and hence may cause end-stop collision. Studies on minimum stiffness in terms of seat position [3] and nonlinear stiffness [4] have been conducted to compromise ride comfort and suspension deflection limitation. With the development of magnetorheological (MR) or electrorheological (ER) dampers, semi-active control of seat suspension has been proposed to provide variable damping force with less power consumption [1, 5]. However, either ER fluid or MR fluid only has controllable-damping capability such that the system is only effective during energy dissipation stage. The study on active seat suspension mainly focuses on developing advanced control strategies or applying different types of actuators to improve seat suspension per-

formance with taking account of issues like actuator saturation, load variation, time delay, and reliability, etc. [6, 7, 8, 9, 10, 11]. Among these three types of seat suspensions, active seat suspension is able to provide the best ride comfort performance, and therefore, receives much more attention in recent years.

In addition to seat suspension, vehicle suspension has been extensively studied for a long time [12]. Vehicle suspension is, in fact, designed as a primary suspension for all the vehicles to provide ride comfort, road holding, and other dynamic functions. Similar to seat suspension, passive, semi-active, and active vehicle suspensions have also been proposed. Active and semi-active suspensions attracted more attention in both academia and industry for improving vehicle ride comfort and road holding [13, 14, 15]. In particular, the active electromagnetic suspension system presents an impressive perspective for the implementation of active suspension to passenger vehicles [16, 17, 18, 19, 20]. However, it is noticed that most of the current active/semi-active seat suspension and active/semi-active vehicle suspension are designed/studied separately though their common function is to improve vehicle ride comfort performance. It is therefore naturally to think about the question: should they be controlled integrally to provide an enhanced ride comfort performance? This motivates the present study.

To achieve an enhanced ride comfort performance, an integrated seat and suspension model which includes a quarter-car suspension (2 degree-of-freedom (DOF)), a seat suspension (2 DOF), and a driver body model (4 DOF) is developed in this paper at first. Developing such an integrated model is twofold: (1) it will be used to design an integrated controller which provides control forces to both car suspension and seat suspension; (2) typical road disturbances can be applied to vehicle tyre instead of cabin to evaluate the suspension performance. This is more reasonable because road signals must be filtered by vehicle suspension in both amplitude and frequency components when getting to the cabin. Directly applying typical road disturbances to cabin to evaluate seat suspension performance may not be appropriate, in particular, when studying issues like actuator saturation and suspension deflection limitation, which are generally subject to the applied

inputs. In addition, suspension performance on ride comfort can be evaluated in terms of human body model instead of sprung mass because sprung mass acceleration cannot fully reflect human body biomechanical effect on ride comfort. Up to date, only a few studies [21, 22] consider both vehicle suspension and seat suspension together to study vehicle or seat suspension optimisation problem. Based on the integrated model, a H_∞ state feedback controller is then designed for the integrated seat and suspension model to generate desired control forces for reducing driver head acceleration under energy bounded road inputs and actuator saturation constraints. Then, a static output feedback controller is designed with considering that not all the state variables, in particular, the state variables in relation to the human body model, are not measurement available in practice. And then, a robust controller design which considers parameter uncertainties and performance requirements on suspension stroke and road holding properties is further discussed. At last, numerical simulations are used to validate the effectiveness of the proposed control strategy by comparing it with passive seat and suspension, active seat suspension control, and active car suspension control.

This paper is organised as follows. In Section 2, the integrated seat and suspension model is developed. In Section 3, the controller design approaches for the proposed model will be presented, where a controller design procedure for a nominal system with one objective on ride comfort is discussed at first, and then, a robust controller design for an uncertain system with three objectives is further discussed. The simulation results will be shown in Section 4. Finally, conclusions are summarised in Section 5.

The notation used throughout the paper is standard. For a real symmetric matrix W, the notation of $W > 0$ ($W < 0$) is used to denote its positive- (negative-) definiteness. $\|\cdot\|$ refers to either the Euclidean vector norm or the induced matrix 2-norm. I is used to denote the identity matrix of appropriate dimensions. To simplify notation, $*$ is used to represent a block matrix which is readily inferred by symmetry.

c_{ss}	damping of seat suspension	k_{ss}	stiffness of seat suspension
c_c	damping of seat cushion	k_c	stiffness of seat cushion
c_1	damping of buttocks and thighs	k_1	stiffness of buttocks and thighs
c_2	damping of lumber spine	k_2	stiffness of lumber spine
c_3	damping of thoracic spine	k_3	stiffness of thoracic spine
c_4	damping of cervical spine	k_4	stiffness of cervical spine

Table 1: Parameters of the seat-driver suspension model

2 Integrated Vehicle Seat and Suspension Model

The integrated vehicle seat and suspension model includes a quarter-car suspension model, a seat suspension model, and a four DOF driver body model as shown in Figure 1, where m_s is the sprung mass, which represents the car chassis; m_u is the unsprung mass, which represents the wheel assembly; m_f is the seat frame mass; m_c is the seat cushion mass; the driver body is composed of four mass segments, i.e., thighs m_1, lower torso m_2, high torso m_3, and head m_4, where arms and legs are combined with the upper torso and thighs, respectively. z_u, z_s, z_f, z_c, and $z_{1\sim4}$ are the displacements of the corresponding masses, respectively; z_r is the road displacement input. c_s and k_s are damping and stiffness of the car suspension system, respectively; k_t and c_t stand for compressibility and damping of the pneumatic tyre, respectively; c_s, c_{ss}, $c_{1\sim4}$, k_s, k_{ss}, and $k_{1\sim4}$ are defined in Table 49. u_s and u_f represent the active control forces applied to the car suspension and the seat suspension, respectively. In practice, electro-hydraulic actuators or linear permanent magnet motors could be applied to generate the required forces u_s and u_f.

The dynamic vertical motion of equations for the quarter-car suspension, seat suspension, and driver body are given by

$$m_u\ddot{z}_u = -k_t(z_u - z_r) - c_t(\dot{z}_u - \dot{z}_r) + k_s(z_s - z_u) + c_s(\dot{z}_s - \dot{z}_u) + u_s, \quad (1)$$

$$m_s\ddot{z}_s = -k_s(z_s - z_u) - c_s(\dot{z}_s - \dot{z}_u) + k_{ss}(z_f - z_s) + c_{ss}(\dot{z}_f - \dot{z}_s) - u_s + u_f, \quad (2)$$

$$m_f\ddot{z}_f = -k_{ss}(z_f - z_s) - c_{ss}(\dot{z}_f - \dot{z}_s) + k_c(z_c - z_f) + c_c(\dot{z}_c - \dot{z}_f) - u_f, \quad (3)$$

$$m_c\ddot{z}_c = -k_c(z_c - z_f) - c_c(\dot{z}_c - \dot{z}_f) + k_1(z_1 - z_c) + c_1(\dot{z}_1 - \dot{z}_c), \quad (4)$$

$$m_1\ddot{z}_1 = -k_1(z_1 - z_c) - c_1(\dot{z}_1 - \dot{z}_c) + k_2(z_2 - z_1) + c_2(\dot{z}_2 - \dot{z}_1), \quad (5)$$

$$m_2\ddot{z}_2 = -k_2(z_2 - z_1) - c_2(\dot{z}_2 - \dot{z}_1) + k_3(z_3 - z_2) + c_3(\dot{z}_3 - \dot{z}_2), \quad (6)$$

$$m_3\ddot{z}_3 = -k_3(z_3 - z_2) - c_3(\dot{z}_3 - \dot{z}_2) + k_4(z_4 - z_3) + c_4(\dot{z}_4 - \dot{z}_3), \quad (7)$$

$$m_4\ddot{z}_4 = -k_4(z_4 - z_3) - c_4(\dot{z}_4 - \dot{z}_3). \quad (8)$$

Note that the quarter-car suspension model (1)–(2) with $k_{ss} = 0$, $c_{ss} = 0$, and $u_f = 0$ has been used by many researchers in studying active or semi-active control of vehicle suspensions. The seat suspension model (3)–(4) or seat suspension with driver body model (3)–(8) with $k_s = 0$, $c_s = 0$, and $z_s = z_r$ has been applied in studying active or semi-active seat suspension control. An integrated model (1)–(3) or (1)–(4) with $u_s = 0$ and $u_f = 0$ have been used in studying seat or suspension optimisation problem [21, 22]. Up to the date, no integrated model (1)–(8) has been found in the literature to study active seat and suspension control together.

By defining the following set of state variables

$x_1 = z_u - z_r$, $x_2 = \dot{z}_u$, $x_3 = z_s - z_u$, $x_4 = \dot{z}_s$, $x_5 = z_f - z_s$, $x_6 = \dot{z}_f$, $x_7 = z_c - z_f$, $x_8 = \dot{z}_c$, $x_9 = z_1 - z_c$, $x_{10} = \dot{z}_1$, $x_{11} = z_2 - z_1$, $x_{12} = \dot{z}_2$, $x_{13} = z_3 - z_2$, $x_{14} = \dot{z}_3$, $x_{15} = z_4 - z_3$, $x_{16} = \dot{z}_4$, the state vector

$$x = \begin{bmatrix} x_1 & x_2 & x_3 & x_4 & x_5 & x_6 & x_7 & x_8 & x_9 & x_{10} & x_{11} & x_{12} & x_{13} & x_{14} & x_{15} & x_{16} \end{bmatrix}^T,$$

the control input vector

$$u = \begin{bmatrix} u_f & u_s \end{bmatrix}^T,$$

and the road disturbance $w = \dot{z}_r$, we can write the dynamic equations (1)–(8) into a state-space form as

$$\dot{x} = Ax + B_w w + Bu, \quad (9)$$

where matrices A, B_w, and B can be obtained from (1)–(8).

In practice, all the actuators are limited by their physical capabilities, and hence, actuator saturation needs to be considered for active control of seat suspension [10] and

car suspension [23]. Taking actuator saturation into account, equation (9) is modified as

$$\dot{x} = Ax + B_w w + B\bar{u}, \tag{10}$$

where $\bar{u}$ =sat(u), and sat(u) is a saturation function of control input u defined as

$$\text{sat}(u) = \begin{cases} -u_{\text{lim}} & \text{if } u < -u_{\text{lim}}, \\ u & \text{if } -u_{\text{lim}} \leqslant u \leqslant u_{\text{lim}}, \\ u_{\text{lim}} & \text{if } u > u_{\text{lim}}, \end{cases} \tag{11}$$

where u_{lim} is the control input limit.

To deal with the saturation problem in the controller design process, the following lemma will be used.

Lemma 1 *[24] For the saturation constraint defined by (11), as long as* $|u| \leqslant \frac{u_{\text{lim}}}{\varepsilon}$, *we have*

$$\left\| \bar{u} - \frac{1+\varepsilon}{2} u \right\| \leqslant \frac{1-\varepsilon}{2} \|u\|, \tag{12}$$

and hence,

$$\left[\bar{u} - \frac{1+\varepsilon}{2} u \right]^T \left[\bar{u} - \frac{1+\varepsilon}{2} u \right] \leqslant \left(\frac{1-\varepsilon}{2} \right)^2 u^T u, \tag{13}$$

where $0 < \varepsilon < 1$ *is a given scalar.*

To apply Lemma 1 in the next section, system (10) is further written as

$$\begin{aligned} \dot{x} &= Ax + B_w w + B\frac{1+\varepsilon}{2} u + B\left(\bar{u} - \frac{1+\varepsilon}{2} u \right) \\ &= Ax + B_w w + B\frac{1+\varepsilon}{2} u + Bv, \end{aligned} \tag{14}$$

where $v = \bar{u} - \frac{1+\varepsilon}{2} u$.

To derive the main result, the following lemma is also used.

Lemma 2 *[25] For any matrices (or vectors)* X *and* Y *with appropriate dimensions, we have*

$$X^T Y + Y^T X \leqslant \epsilon X^T X + \epsilon^{-1} Y^T Y, \tag{15}$$

where $\epsilon > 0$ *is any scalar.*

3 Controller Design

To improve the system performance, a state feedback controller is designed as

$$u = Kx, \tag{16}$$

where K is the feedback gain matrix to be designed. It can be seen that the input to the controller is the state vector x and the output of the controller is the control force vector u, which is also the control input to the system (10). Once K is known, u can be calculated by using (16). For further understanding this, Figure 1 shows a block diagram of the controller of which inputs are the state variables x_1 to x_8, which are assumed to be measurable in practice as an example, and outputs are u_s and u_f.

For car and seat suspension design, the performance on ride comfort is mainly described by the driver head acceleration [9, 11], and therefore, the driver head acceleration,

$$z = \ddot{z}_4 = Cx, \tag{17}$$

where C is the last row of A matrix, is defined as the control output.

To achieve good ride comfort and make the controller performing adequately for a wide range of road disturbances, the L_2 gain between the road disturbance input w and the control output z, which is defined as

$$\|T_{zw}\|_\infty = \sup_{w \neq 0} \frac{\|z\|_2}{\|w\|_2}, \tag{18}$$

where $\|z\|_2^2 = \int_0^\infty z^T(t)z(t)dt$ and $\|w\|_2^2 = \int_0^\infty w^T(t)w(t)dt$, is chosen as the performance measure. A small value of $\|T_{zw}\|_\infty$ generally means a small value of driver head acceleration under the energy limited road disturbances. Therefore, the control objective is to design a controller (16) such that the closed-loop system, which is composed by substituting (16) into (10), is asymptotically stable, and the performance measure (18) is minimised.

3.1 Controller Design for A Nominal System

To design such a controller, we now define a Lyapunov function for system (10), which is assumed to be a nominal system without parameter uncertainties, as

$$V(x) = x^T P x \tag{19}$$

where P is a positive definite matrix. By differentiating (19) and using (14), we obtain

$$\begin{aligned}
\dot{V}(x) &= \dot{x}^T P x + x^T P \dot{x} \\
&= \left[Ax + B_w w + B\frac{1+\varepsilon}{2}u + Bv \right]^T Px \\
&\quad + x^T(t) P \left[Ax + B_w w + B\frac{1+\varepsilon}{2}u + Bv \right].
\end{aligned} \tag{20}$$

By using Lemma 1, Lemma 2, and equation (16), we have

$$\begin{aligned}
\dot{V}(x) &\leqslant x^T \left[A^T P + PA + \left(B\frac{1+\varepsilon}{2}K \right)^T P + PB\frac{1+\varepsilon}{2}K \right] x \\
&\quad + w^T B_w^T P x + x^T P B_w w + \epsilon v^T v + \epsilon^{-1} x^T P B B^T P x \\
&\leqslant x^T \left[A^T P + PA + \left(B\frac{1+\varepsilon}{2}K \right)^T P + PB\frac{1+\varepsilon}{2}K \right] x + w^T B_w^T P x \\
&\quad + x^T P B_w w + \epsilon \left(\frac{1-\varepsilon}{2} \right)^2 u^T u + \epsilon^{-1} x^T P B B^T P x \\
&= x^T \Theta x + w^T B_w^T P x + x^T P B_w w,
\end{aligned} \tag{21}$$

where

$$\Theta = \left[A^T P + PA + \left(B\frac{1+\varepsilon}{2}K \right)^T P + PB\frac{1+\varepsilon}{2}K + \epsilon \left(\frac{1-\varepsilon}{2} \right)^2 K^T K + \epsilon^{-1} P B B^T P \right],$$

and ϵ is any positive scalar.

Adding $z^T z - \gamma^2 w^T w$, $\gamma > 0$ is a performance index, to the two sides of (21) yields

$$\begin{aligned}
&\dot{V}(x) + z^T z - \gamma^2 w^T w \\
&\leqslant \begin{bmatrix} x^T & w^T \end{bmatrix} \begin{bmatrix} \Theta + C^T C & P B_w \\ B_w^T P & -\gamma^2 I \end{bmatrix} \begin{bmatrix} x \\ w \end{bmatrix} \\
&= \begin{bmatrix} x^T & w^T \end{bmatrix} \Pi \begin{bmatrix} x \\ w \end{bmatrix},
\end{aligned} \tag{22}$$

where $\Pi = \begin{bmatrix} \Theta + C^T C & PB_w \\ B_w^T P & -\gamma^2 I \end{bmatrix}$.

It is now deduced from (22) that if $\Pi < 0$, then, $\dot{V}(x) + z^T z - \gamma^2 w^T w < 0$, and then, $\|T_{zw}\|_\infty < \gamma$ with the initial condition $x(0) = 0$ [26]. When the road disturbance is zero, i.e., $w = 0$, it can be inferred from (22) that if $\Pi < 0$, then $\dot{V}(x) < 0$, and the system (10) with the controller (16) is quadratically stable.

By pre- and post-multiplying Π with $\mathrm{diag}\begin{pmatrix} P^{-1} & I \end{pmatrix}$ and its transpose, respectively, and defining $Q = P^{-1}$ and $Y = KQ$, the condition of $\Pi < 0$ is equivalent to

$$\begin{bmatrix} QA^T + AQ + \frac{1+\varepsilon}{2} Y^T B^T + \frac{1+\varepsilon}{2} BY & B_w \\ +\epsilon \left(\frac{1-\varepsilon}{2}\right)^2 Y^T Y + \epsilon^{-1} BB^T + QC^T CQ & \\ B_w^T & -\gamma^2 I \end{bmatrix} < 0. \tag{23}$$

By the Schur complement, (23) is equivalent to

$$\begin{bmatrix} QA^T + AQ + \frac{1+\varepsilon}{2}\left[Y^T B^T + BY\right] + \epsilon^{-1} BB^T & Y^T & QC^T & B_w \\ * & -\epsilon^{-1}\left(\frac{2}{1-\varepsilon}\right)^2 I & 0 & 0 \\ * & * & -I & 0 \\ * & * & * & -\gamma^2 I \end{bmatrix} < 0. \tag{24}$$

On the other hand, from (16), the constraint $|u| \leqslant \frac{u_{\lim}}{\varepsilon}$ can be expressed as

$$|Kx| \leqslant \frac{u_{\lim}}{\varepsilon}. \tag{25}$$

Let $\Omega(K) = \left\{x| \ |x^T K^T K x| \leqslant \left(\frac{u_{\lim}}{\varepsilon}\right)^2\right\}$, the equivalent condition for an ellipsoid $\Omega(P, \rho) = \left\{x| \ x^T P x \leqslant \rho\right\}$ being a subset of $\Omega(K)$, i.e., $\Omega(P, \rho) \subset \Omega(K)$, is given as [27]

$$K \left(\frac{P}{\rho}\right)^{-1} K^T \leqslant \left(\frac{u_{\lim}}{\varepsilon}\right)^2. \tag{26}$$

By the Schur complement, inequality (26) can be written as

$$\begin{bmatrix} \left(\frac{u_{\lim}}{\varepsilon}\right)^2 I & K\left(\frac{P}{\rho}\right)^{-1} \\ \left(\frac{P}{\rho}\right)^{-1} K^T & \left(\frac{P}{\rho}\right)^{-1} I \end{bmatrix} \geqslant 0. \tag{27}$$

Using the definitions $Q = P^{-1}$, and $Y = KQ$, inequality (27) is equivalent to

$$\begin{bmatrix} \left(\frac{u_{\lim}}{\varepsilon}\right)^2 I & Y \\ Y^T & \rho^{-1}Q \end{bmatrix} \geqslant 0. \tag{28}$$

The controller design problem is now summarised as: for given numbers $\gamma > 0$, $\varepsilon > 0$, $\rho > 0$ and $u_{\lim}$, the system (10) with controller (16) is quadratically stable and $\|T_{zw}\|_\infty < \gamma$ if there exist matrices $Q > 0$, Y, and scalar $\epsilon > 0$ such that linear matrix inequalities (LMIs) (24), (28) and (54) are feasible. Moreover, the feedback gain matrix is obtained as $K = YQ^{-1}$.

It is noticed that (24) and (28) are LMIs to γ^2, hence, to minimise the performance measure γ, the controller design problem can be modified as a minimisation problem of

$$\min\ \gamma^2 \qquad \text{s.t.} \qquad \text{LMIs (24) and (28).} \tag{29}$$

This minimisation problem is a convex optimisation problem and can be solved by using some available software such as Matlab LMI Toolbox. Since the solution to (29) will be dependent on the values of ε and ρ, it is a sub-optimal solution for a given $u_{\lim}$. Choosing values for ε and ρ is a trial and error process. In general, using small values of ε and ρ may get a high gain controller design.

It is noted that the above-designed state feedback controller assumes that all the state variables are measurement available. This is not true, in particular, when considering high DOF human body model where most of the state variables, such as torso displacements and velocities, etc., are not measurable or not suitable for measurement when a driver is driving. Therefore, a control strategy which only uses available measurements needs to be developed. An observer-based output feedback or dynamic output feedback [11] could be applied with using the available measurements, however, it makes the design and implementation tasks expensive and hard, in particular, when the model order (even after model reduction [5]) is higher. On the contrary, controllers using static output feedback are less expensive to implement and are more reliable. Therefore, a static output feedback controller will be further considered for the integrated seat and suspension control. Static

output feedback controller is a challenging issue from both analytical and numerical points of view due to its non-convex nature [28]. Although genetic algorithms (GAs) can be applied to design a static output feedback controller [29], a computationally efficient numerical algorithm [30] will be applied here.

The static output feedback controller is designed as

$$u = KC_s x \tag{30}$$

where C_s is used to define the available state variables. For example, if only x_1 in (9) is available for feedback, then C_s is defined as $C_s = \begin{bmatrix} 1 & [0]_{1\times 15} \end{bmatrix}$.

By using (30) instead of (16) in (20), defining $WC_s = C_sQ$ and $Y = KW$, and following similar procedure as derived for state feedback controller design, we can get the following conditions, which are similar to (24) and (28), respectively, for the static output feedback controller design

$$\begin{bmatrix} QA^T + AQ + \frac{1+\varepsilon}{2}\left[C_s^T Y^T B^T + BYC_s\right] + \epsilon^{-1}BB^T & C_s^T Y^T & QC^T & B_w \\ * & -\epsilon^{-1}\left(\frac{2}{1-\varepsilon}\right)^2 I & 0 & 0 \\ * & * & -I & 0 \\ * & * & * & -\gamma^2 I \end{bmatrix} < 0, \tag{31}$$

$$\begin{bmatrix} \left(\frac{u_{\lim}}{\varepsilon}\right)^2 & YC_s \\ C_s^T Y^T & \rho^{-1}Q \end{bmatrix} \geqslant 0, \tag{32}$$

and the static output feedback gain matrix is obtained as $K = YW^{-1}$.

It is observed that the static output feedback controller design is the feasibility problem of LMIs (7) and (32) with equality constraint $WC_s = C_sQ$. The equality constraint $WC_s = C_sQ$ can be equivalently converted to [31]

$$\mathrm{tr}\left[(WC_s - C_sQ)^T (WC_s - C_sQ)\right] = 0. \tag{33}$$

By introducing the condition

$$(WC_s - C_sQ)^T (WC_s - C_sQ) \leqslant \mu I, \tag{34}$$

where $\mu > 0$, it is then equivalent to

$$\begin{bmatrix} -\mu I & (WC_s - C_sQ)^T \\ WC_s - C_sQ & -I \end{bmatrix} \leqslant 0, \tag{35}$$

by means of the Schur complement. If we assume μ as a very small positive number, say for example 10^{-10}, then we can numerically design a static output feedback controller by solving the following minimisation problem

$$\min\ \gamma^2 \qquad \text{s.t.} \qquad \text{to LMIs (31), (32), and (35).} \tag{36}$$

3.2 Robust Multiobjective Controller Design

In practice, the mass of the driver body may be varied when a driver's physical condition is changed or a different driver who has a different weight is driving the vehicle. To make the controller have similar performance despite the changes of driver's mass, the variation to the driver's mass will be considered. Referring to the driver model used in this paper, it can be seen that the driver's mass is composed of the masses of thighs, lower torso, high torso, and head, i.e., $m = \sum_{i=1}^{4} m_i$. It is reasonable to assume that the mass variation ratio to each segment of the driver body is equal and the driver's mass is actually varied in a range of $[m_{\min}, m_{\max}]$, where $m_{\min}$ and $m_{\max}$ are the possible minimum and maximum driver masses, respectively. Therefore, it is not difficult to represent the uncertain driver mass appeared in the model as

$$\frac{1}{m} = h_1 \frac{1}{m_{\min}} + h_2 \frac{1}{m_{\max}}, \tag{37}$$

where h_1 and h_2 are defined as

$$h_1 = \frac{1/m - 1/m_{\max}}{1/m_{\min} - 1m_{\max}},\ h_2 = \frac{1/m_{\max} - 1/m}{1/m_{\min} - 1/m_{\max}}. \tag{38}$$

It can be seen that $h_i \geqslant 0$, $i = 1, 2$, and $\sum_{i=1}^{2} h_i = 1$. If we define $m_{\min} = (1-\delta)m = \delta_{\min} m = \delta_{\min} \sum_{i=1}^{4} m_i$, $m_{\max} = (1+\delta)m = \delta_{\max} m = \delta_{\max} \sum_{i=1}^{4} m_i$, where $0 < \delta < 1$, $\delta_{\min} = 1 - \delta$, and $\delta_{\max} = 1 + \delta$, the vehicle model in (10) with uncertain driver mass can

be expressed as

$$\dot{x} = \sum_{i=1}^{2} h_i A_i x + B_w w + B\bar{u}, \tag{39}$$

where matrices A_i, $i = 1, 2$, are obtained by replacing m_j, $j = 1, 2, 3, 4$ in matrix A with $\delta_{\min} m_j$ and $\delta_{\max} m_j$, respectively.

On the other hand, parameter uncertainties may happen to the damping coefficient and stiffness of each segment of driver body, of which values are in fact hard to be measured accurately in practice. To describe these uncertainties in the model, a norm-bounded method can be used. If we assume the stiffness and damping coefficient with uncertainties can be described as $k = k_o(1 + d_k\delta_k)$ and $c = c_o(1 + d_c\delta_c)$, respectively, where k_o and c_o are the nominal values, δ_k and δ_c are the uncertainties with $|\delta_k| \leqslant 1$ and $|\delta_c| \leqslant 1$, and d_k (d_c) indicates the percentage of variation that is allowed for a given parameter around its nominal value, then, taking a matrix T with uncertain k and c as an example, it can be expressed as

$$\begin{aligned} T &= \begin{bmatrix} k & c \\ \# & \# \end{bmatrix} = \begin{bmatrix} k_o(1 + d_k\delta_k) & c_o(1 + d_c\delta_c) \\ \# & \# \end{bmatrix} \\ &= \begin{bmatrix} k_o & c_o \\ \# & \# \end{bmatrix} + \begin{bmatrix} 1 & 1 \\ 0 & 0 \end{bmatrix} \begin{bmatrix} \delta_k & 0 \\ 0 & \delta_c \end{bmatrix} \begin{bmatrix} d_k k_o & 0 \\ 0 & d_c c_o \end{bmatrix} \\ &= T_o + HFE, \end{aligned}$$

where $T_o = \begin{bmatrix} k_o & c_o \\ \# & \# \end{bmatrix}$, $H = \begin{bmatrix} 1 & 1 \\ 0 & 0 \end{bmatrix}$, $E = \begin{bmatrix} d_k k_o & 0 \\ 0 & d_c c_o \end{bmatrix}$, $F = \begin{bmatrix} \delta_k & 0 \\ 0 & \delta_c \end{bmatrix}$ with $F^T F \leqslant I$, $\#$ represents an arbitrary element in the matrix. Following the similar principle, the system (39) with parameter uncertainties on stiffnesses and damping coefficients can be actually expressed as

$$\dot{x} = \sum_{i=1}^{2} h_i(A_i + \Delta A_i)x + B_w w + B\bar{u}, \tag{40}$$

where $\Delta A_i = H_a F E_i$ represents the uncertainty caused by the uncertain stiffnesses and damping coefficients on matrix A_i, H_a and E_i are known constant matrices with appropriate dimensions, which can be defined in terms of the locations and variation ranges

of the uncertain parameters appeared in the matrix A_i, and F is an unknown matrix function bounded by $F^TF \leqslant I$. For description simplicity, we define $A_h = \sum_{i=1}^{2} h_i A_i$, $\Delta A_h = \sum_{i=1}^{2} h_i \Delta A_i = \sum_{i=1}^{2} h_i H_a F E_i = H_a F E_h$,where $E_h = \sum_{i=1}^{2} h_i E_i$, and $\hat{A}_h = A_h + \Delta A_h$, then, (40) is expressed as

$$\dot{x} = \hat{A}_h x + B_w w + B\bar{u}. \tag{41}$$

Similarly, the control output (17) can be expressed as

$$z = \ddot{z}_4 = \hat{C}_h x, \tag{42}$$

where $\hat{C}_h = C_h + \Delta C_h$, $C_h = \sum_{i=1}^{2} h_i C_i$, $\Delta C_h = \sum_{i=1}^{2} h_i \Delta C_i = \sum_{i=1}^{2} h_i H_c F E_i = H_c F E_h$.

Note that the parameter uncertainties on stiffnesses and damping coefficients of car and seat suspensions, sprung and unsprung masses, etc., can be dealt with in a same way, which, however, will not be further discussed here.

For the uncertain system (41) and the control output (42), the condition (31) is also applied and can be obtained as

$$\begin{bmatrix} Q\hat{A}_h^T + \hat{A}_h Q + \frac{1+\varepsilon}{2}\left[C_s^T Y^T B^T + BYC_s\right] + \epsilon^{-1}BB^T & C_s^T Y^T & Q\hat{C}_h^T & B_w \\ * & -\epsilon^{-1}\left(\frac{2}{1-\varepsilon}\right)^2 I & 0 & 0 \\ * & * & -I & 0 \\ * & * & * & -\gamma^2 I \end{bmatrix} < 0, \tag{43}$$

which is further expressed as

$$\begin{bmatrix} Q(A_h + \Delta A_h)^T + (A_h + \Delta A_h)Q \\ +\frac{1+\varepsilon}{2}\left[C_s^T Y^T B^T + BYC_s\right] + \epsilon^{-1}BB^T & C_s^T Y^T & Q(C_h + \Delta C_h)^T & B_w \\ * & -\epsilon^{-1}\left(\frac{2}{1-\varepsilon}\right)^2 I & 0 & 0 \\ * & * & -I & 0 \\ * & * & * & -\gamma^2 I \end{bmatrix} < 0. \tag{44}$$

We now need the following lemma to derive the result.

Lemma 3 *[32] Given appropriately dimensioned matrices* Σ_1, Σ_2, Σ_3, *with* $\Sigma_1^T = \Sigma_1$, *then*

$$\Sigma_1 + \Sigma_3\Delta\Sigma_2 + \Sigma_2^T\Delta\Sigma_3^T < 0$$

holds for all Δ *satisfying* $\Delta^T\Delta \leq I$ *if and only if for* $\epsilon > 0$

$$\Sigma_1 + \epsilon\Sigma_3\Sigma_3^T + \epsilon^{-1}\Sigma_2^T\Sigma_2 < 0.$$

In fact, inequality (44) is equivalent to

$$\Sigma_1 + \Sigma_3 F\Sigma_2 + \Sigma_2^T F\Sigma_3^T < 0, \tag{45}$$

where

$$\Sigma_1 = \begin{bmatrix} QA_h^T + A_hQ + \frac{1+\varepsilon}{2}\left[C_s^TY^TB^T + BYC_s\right] + \epsilon^{-1}BB^T & C_s^TY^T & QC_h^T & B_w \\ * & -\epsilon^{-1}\left(\frac{2}{1-\varepsilon}\right)^2 I & 0 & 0 \\ * & * & -I & 0 \\ * & * & * & -\gamma^2 I \end{bmatrix},$$

$\Sigma_3^T = \begin{bmatrix} H_a^T & 0 & H_c^T & 0 \end{bmatrix}$, $\Sigma_2 = \begin{bmatrix} E_hQ & 0 & 0 & 0 \end{bmatrix}$. By using Lemma 3, we can see that the inequality (45) is satisfied if the following inequality holds for $\epsilon_1 > 0$

$$\begin{bmatrix} QA_h^T + A_hQ & & & & \\ +\frac{1+\varepsilon}{2}\left[C_s^TY^TB^T + BYC_s\right] & C_s^TY^T & QC_h^T & B_w & QE_h^T \\ +\epsilon^{-1}BB^T + \epsilon_1^{-1}H_aH_a^T & & +\epsilon_1^{-1}H_aH_c^T & & \\ * & -\epsilon^{-1}\left(\frac{2}{1-\varepsilon}\right)^2 I & 0 & 0 & 0 \\ * & * & -I & 0 & 0 \\ * & * & * & -\gamma^2 I & 0 \\ * & * & * & * & -\epsilon_1^{-1}I \end{bmatrix} < 0. \tag{46}$$

By the definitions $A_h = \sum_{i=1}^{2} h_iA_i$, $E_h = \sum_{i=1}^{2} h_iE_i$, and the fact that $h_i \geqslant 0$ and $\sum_{i=1}^{2} h_i = 1$,

(46) is equivalent to

$$\begin{bmatrix} QA_i^T + A_iQ \\ +\frac{1+\varepsilon}{2}\left[C_s^T Y^T B^T + BYC_s\right] \\ +\epsilon^{-1}BB^T + \epsilon_1^{-1}H_aH_a^T & C_s^T Y^T & QC_i^T + \\ & & \epsilon_1^{-1}H_aH_c^T & B_w & QE_i^T \\ * & -\epsilon^{-1}\left(\frac{2}{1-\varepsilon}\right)^2 I & 0 & 0 & 0 \\ * & * & -I & 0 & 0 \\ * & * & * & -\gamma^2 I & 0 \\ * & * & * & * & -\epsilon_1^{-1}I \end{bmatrix} < 0 \quad (47)$$

$$i = 1, 2.$$

In addition, it is noticed that in the above mentioned design, the driver's ride comfort is regarded as a main goal to be optimised and the vehicle suspension control is employed to achieve this goal. However, with relying on the car suspension control to optimise the head acceleration, it may possibly worsen car suspension stroke, seat suspension stroke, and road holding properties. Therefore, the car suspension stroke limitation, seat suspension stroke limitation, and the road holding capability should be considered in the controller design procedure as well. This is becoming a multiobjective control problem, where the following constraints should be satisfied while the ride comfort performance is optimised

$$|z_s - z_u| \leqslant z_{\max 1}, \quad (48)$$

$$|z_f - z_s| \leqslant z_{\max 2}, \quad (49)$$

and

$$k_t(z_u - z_r) < 9.8(m_s + m_u), \quad (50)$$

where $z_{\max 1}$ is the maximum car suspension stroke hard limit, $z_{\max 2}$ is the maximum seat suspension stroke hard limit, and constraint (50) means that the dynamic tyre load should be less than the static tyre load so that the wheel can be kept contact with the ground.

To deal with these constraints, the car suspension stroke, seat suspension stroke, and

tyre load are defined as another control output, i.e.,

$$z_2 = \begin{bmatrix} \alpha_1(z_s - z_u)/z_{\max 1} \\ \alpha_2(z_f - z_s)/z_{\max 2} \\ \alpha_3 k_t(z_u - z_r)/9.8(m_{s\min} + m_u) \end{bmatrix} = C_c x, \tag{51}$$

where $C_c = \begin{bmatrix} 0 & 0 & \alpha_1/z_{\max 1} & 0 & 0 & \\ 0 & 0 & 0 & 0 & \alpha_2/z_{\max 2} & \mathbf{0}_{3\times 11} \\ \alpha_3 k_t/9.8(m_{s\min} + m_u) & 0 & 0 & 0 & 0 & \end{bmatrix}$, α_1, α_2, and α_3 are weighting parameters, and the performance, $\|z_2\|_\infty < \gamma \|w\|_2$, is required to be realised, where $\|z\|_\infty \triangleq \sup_{t\in[0,\infty)} \sqrt{z^T(t)z(t)}$ and $\gamma > 0$ is a performance index. It is noted that the weighting parameters α_1, α_2, and α_3 can be properly chosen to provide the trade-off among different requirements such as ride comfort and road holding [33]. In general, if a small suspension stroke is required, a big weighting value for α_1 or α_2 should be chosen; if good road holding performance is required, a big value for α_3 should be chosen.

By using the Schur complement, the feasibility of the following inequality

$$\begin{bmatrix} P & C_c^T \\ C_c & I \end{bmatrix} > 0 \tag{52}$$

guarantees $C_c^T C_c < P$. At the same time, it can be derived from (19) and (22) that $x^T P x < \gamma^2 \int_0^t w^T(s)w(s)ds$ if $\Pi < 0$ is guaranteed. Then, it can be easily established from (51) and (52) that for all $t \geqslant 0$,

$$z_2^T z_2 = x^T C_c^T C_c x < x^T P x < \gamma^2 \int_0^t w^T(s)w(s)ds \leqslant \gamma^2 \int_0^\infty w^T(s)w(s)ds. \tag{53}$$

Taking the supremum over $t \geqslant 0$ yields $\|z_2\|_\infty < \gamma \|w\|_2$ for all $w \in L_2[0,\infty)$.

Pre- and post-multiplying (52) by $\mathrm{diag}\begin{pmatrix} P^{-1} & I \end{pmatrix}$ and its transpose, respectively, and defining $Q = P^{-1}$, the condition (52) is equivalent to

$$\begin{bmatrix} Q & QC_c^T \\ C_c Q & I \end{bmatrix} > 0. \tag{54}$$

Considering parameter uncertainties and the multiobjective control requirement, we now summarise the robust multiobjective controller design problem as: for given scalars $\rho > 0$, $\varepsilon > 0$, matrices H_a, H_c, E_i, $i = 1, 2$, the uncertain system (41) with controller (30) is quadratically stable and the L_2 gain defined by (18) is less than γ and $\|z_2\|_\infty < \gamma \|w\|_2$ if there exist matrices $Q > 0$, Y, scalars $\epsilon > 0$, $\epsilon_1 > 0$, such that the following minimisation problem is feasible

$$\min \ \gamma^2 \qquad \text{s.t.} \qquad \text{LMIs (32), (35), (47), and (54).} \tag{55}$$

By solving the problem of (55), the controller gain matrix can be obtained as $K = YW^{-1}$.

It is noted that the performance requirement enforced on the control output z_2 is subjected to the performance index γ and the energy of the road disturbance $\|w\|_2$. Even when γ is minimised, the constraints on the suspension stroke and the dynamic tyre load may be deteriorated in practice if the road disturbance is too strong. Nevertheless, when designing a controller, an appropriate weighting on the control output z_2 can provide a good compromise among the ride comfort performance, suspension stroke limitation, and road holding capability.

4 Numerical Simulations

4.1 Validation on A Quarter-Car Model

Numerical simulations are conducted in this section to show the effectiveness of the proposed integrated seat and suspension control for improving driver ride comfort. The parameters used in the simulations are listed in Table 2, where the quarter-car suspension parameters have been optimised in terms of driver body acceleration in [22] and the seat suspension and driver body model parameters are referred to [5].

In the simulation, the actuator force limitation for the quarter-car suspension is considered as 1500 N and for the seat suspension as 500 N. The scalars $\varepsilon = 0.9$ and $\rho = 10^{-3}$

Mass (kg)		Damping coefficient (Ns/m)		Spring stiffness (N/m)	
m_u	20	c_t	0	k_t	180000
m_s	300	c_s	2000	k_s	10000
m_f	15	c_{ss}	830	k_{ss}	31000
m_c	1	c_c	200	k_c	18000
m_1	12.78	c_1	2064	k_1	90000
m_2	8.62	c_2	4585	k_2	162800
m_3	28.49	c_3	4750	k_3	183000
m_4	5.31	c_4	400	k_4	310000

Table 2: Parameter values of the proposed suspension model

are chosen for designing controllers.

To show the effectiveness and advance of the proposed control strategy, several different controllers will be designed and compared. At first, we design a state feedback controller for the seat suspension model only, i.e., equations (3)–(8) with $k_s = 0$ and $c_s = 0$, by solving the minimisation problem of (29) without considering suspension stroke limitation and road holding performance. The obtained controller gain matrix is given as

$$\begin{aligned} K &= 10^6[-2.0237 - 0.0083 - 0.6569 - 0.0079 - 1.0691 - 0.1164 \\ &\quad 1.4845 - 0.0\ 9073.9270 - 0.3336\ 8.3988\ 0.0792]. \end{aligned} \tag{56}$$

This controller will use state variables $x_5 \sim x_{16}$ of the model (9) as feedback signals in the simulation and is denoted as Controller I for description simplicity.

Then, we design another state feedback controller for the quarter-car suspension model only, i.e., equations (1)–(2) with $k_{ss} = 0$, $c_{ss} = 0$ and $u_f = 0$, by solving the minimisation problem of (29) without considering suspension stroke limitation and road holding performance. The obtained controller gain matrix is given as

$$K = 10^3[0.4456\ \ -1.8543\ 9.5208\ 1.1960]. \tag{57}$$

This controller will use state variables $x_1 \sim x_4$ of the model (9) as feedback signals in the

simulation and is denoted as Controller II for description simplicity.

And then, we design a state feedback controller for the integrated seat and suspension model, i.e., equations (1)–(8), by solving the minimisation problem of (29) without considering suspension stroke limitation and road holding performance. The obtained controller gain matrix is given as

$$\begin{aligned} K \;=\; & 10^6[-0.0061 \;-0.0000 \;-0.0052 \;-0.0006\; 0.0198 \;-0.0035\; 0.2834 \;-0.0021 \\ & 0.2195 \;-0.0280\; 0.9059 \;-0.0119\; 1.1534\; 0.0101 \;-26.103\; 0.0284; \\ & 0.0553 \;-0.0001\; 0.0041 \;-0.0096\; 0.1501 - 0.0015\; 0.1983 \;-0.0000 \\ & 0.1636\; 0.0002\; 0.0564\; 0.0021 \;-0.0954\; 0.0162 \;-3.4882 \;-0.0085]. \end{aligned} \tag{58}$$

This controller will use state variables $x_1 \sim x_{16}$ of the model (9) as feedback signals in the simulation and is denoted as Controller III for description simplicity. This controller will provide two control inputs to the seat suspension and car suspension, respectively.

To validate the suspension performance in time-domain, two typical road disturbances, i.e., bump road disturbance and random road disturbance, will be considered in the simulation and applied to the vehicle wheel.

4.1.1 Comparison on Bump Response

The ground displacement for an isolated bump in an otherwise smooth road surface is given by

$$z_r(t) = \begin{cases} \frac{a}{2}(1-\cos(\frac{2\pi v_0}{l}t)), & 0 \leqslant t \leqslant \frac{l}{v_0} \\ 0, & t > \frac{l}{v_0} \end{cases} \tag{59}$$

where a and l are the height and the length of the bump, v_0 is vehicle forward speed. We choose $a = 0.1$ m, $l = 2$ m, and $v_0 = 30$ km/h in the simulation.

The bump responses of the driver head acceleration for the integrated seat and suspension system with different controllers are compared in Figure 2, where Passive means no controller has been used, Active Seat means the Controller I is used for seat suspen-

sion only, Active Suspension means the Controller II is used for car suspension only, and Integrated means the Controller III is used for both seat suspension and car suspension. It can be seen from Figure 2 that the Integrated control achieves the best performance among all the compared control strategies on ride comfort in terms of the peak value of driver head acceleration. Further comparison on the control forces is shown in Figure 3, where the integrated control provides two control forces, which are denoted as Active Seat and Active Suspension to the seat suspension and the car suspension, respectively.

As we discussed above, the state feedback controller is not practically realisable, in particular, when human body model is included. We now design a static output feedback controller for the integrated seat and suspension model (1)–(8) by solving the minimisation problem of (36) without considering suspension stroke limitation and road holding performance. By assuming all the state variables for car suspension and seat suspension are available for measurement by using displacement and velocity sensors or using accelerometers with integration functions, and all the state variable for the driver body model are not measurement available, the controller gain matrix is obtained as

$$K = 10^5 \begin{bmatrix} -0.4665 & 0.0000 & -0.4759 & -0.0080 & -0.1965 & -0.1023 & 8.6420 & -0.1991 \\ 8.2020 & 0.0171 & 1.4630 & -0.1564 & 9.4831 & 0.0284 & 6.1010 & 0.1435 \end{bmatrix} \tag{60}$$

This controller only uses the measurement available state variables $x_1 \sim x_8$ of the model (9) as feedback signals in the simulation and is denoted as Controller IV for description simplicity.

To clearly show the performance of the designed static output feedback controller, the bump responses on driver head acceleration for the integrated seat and suspension system with no controller, state feedback controller, and static output feedback controller are compared in Figure 4, where State Feedback means the Controller III is used and Static Feedback means the Controller IV is used. It can be seen from Figure 4 that the static output feedback controller achieves similar performance to the state feedback controller in terms of the peak value on driver head acceleration in spite of its simple structure. The comparison on the control forces is shown in Figure 5. It can be seen from Figure

5 that both state feedback controller and static output feedback controller provide two control forces to the system, and their forces to seat suspension and car suspension are quite similar.

It is noticed that Controller IV achieves good ride comfort performance with limited information. However, for a vehicle suspension, besides the ride comfort which needs to be focused on, car and seat suspension stroke limitation and road holding performance are also needed to be considered. In addition, parameter uncertainties, which may often happen to the system in practice, will also need be dealt with. Furthermore, the measurement of tyre deflection x_1 and velocity x_2 may not be easily available in practice. Therefore, a robust controller, which compromises the performance among ride comfort, car and seat suspension stroke limitation, and road holding capability, as well as considers parameter uncertainties and measurement availability, is finally designed by solving the problem of (55). The obtained controller gain matrix is given as

$$K = 10^5 \begin{bmatrix} 0.0661 & 0.0065 & -0.2115 & 0.0336 & -2.7173 & -0.0167 \\ -0.1255 & 0.0378 & -0.3292 & -0.0205 & 1.3831 & 0.0042 \end{bmatrix}, \qquad (61)$$

which uses the measurement available state variables $x_3 \sim x_8$ of the model (9) as feedback signals and is denoted as Controller V for description simplicity.

To show the difference between Controller IV and Controller V on different performance aspects, the driver head acceleration, car suspension stroke, seat suspension stroke, and dynamic tyre load under bump road input are shown in Figures 6–9, respectively. It can be seen that Controller IV, which is indicated as Static Feedback in the figures, achieves better ride comfort in terms of the peak value on driver head acceleration in Figure 6 compared to Controller V, which is indicated as Robust Static Feedback. However, it generates bigger suspension stroke and dynamic tyre load as shown in Figures 7 and 9 compared to Controller V. This may cause suspension end-stop collision and wheels lifting off ground. The dynamic tyre load of Controller V is quite similar to the passive suspension in terms of the maximum peak value. Although Controller V requires a bigger seat suspension stroke than Controller IV and passive suspension, it is observed from Figure 8 that the

stroke is still within ±20 mm, which is acceptable for a seat suspension [34]. Therefore, Controller V achieves a good trade-off among different performance requirements. This controller will be further tested on a full-car model in the next subsection.

On the other hand, from implementation point of view, it is noted that for a real vehicle, the above designed controller can be integrated into a Suspension Control Module (SCM) which is designed as an embedded electronic control unit (ECU) that controls one or more of the electrical systems in a car. This module will receive signals from sensors installed at wheels and seat frame, and calculate the required control forces in terms of the designed controller gain matrix. The control forces will then be generated by the actuators and applied to the vehicle and seat. Note that the controller gain matrix is a constant matrix that does not need to be re-calculated in a real-time implementation and can be easily stored in a microprocessor memory (RAM or ROM). The calculation of the control forces is straightforward without high computational power. This enables the implementation of the controller on a microcontroller board.

4.1.2 Comparison on Random Response

When the road disturbance is considered as vibration, it is typically specified as random process with a ground displacement power spectral density (PSD) of

$$S_g(\Omega) = \begin{cases} S_g(\Omega_0)(\frac{\Omega}{\Omega_0})^{-n_1}, & \text{if} \quad \Omega \leq \Omega_0 \\ S_g(\Omega_0)(\frac{\Omega}{\Omega_0})^{-n_2}, & \text{if} \quad \Omega \geq \Omega_0 \end{cases}, \tag{62}$$

where $\Omega_0 = \frac{1}{2\pi}$ is a reference frequency, Ω is a frequency, n_1 and n_2 are road roughness constant. The value $S_g(\Omega_0)$ provides a measure for the roughness of the road. In particular, samples of the random road profile can be generated using the spectral representation method [35]. If the vehicle is assumed to travel with a constant horizontal speed v_0 over a given road, the road irregularities can be simulated by the following series

$$z_r(t) = \sum_{n=1}^{N_f} s_n \sin(n\omega_0 t + \varphi_n), \tag{63}$$

where $s_n = \sqrt{2S_g(n \triangle \Omega) \triangle \Omega}$, $\triangle \Omega = \frac{2\pi}{l}$, l is the length of the road segment, $\omega_0 = \frac{2\pi}{l} v_0$, and φ_n is treated as random variables, following a uniform distribution in the interval $[0,\ 2\pi)$. N_f limits the considered frequency range.

To validate the effectiveness of Controller V under different road conditions and different vehicle speeds, we use $n_1 = 2$, $n_2 = 1.5$, $l = 200$, $N_f = 200$ in equations (62) and (63) and select the road roughness as $S_g(\Omega_0) = 64 \times 10^{-6}$ m^3 (C Grade, Average), $S_g(\Omega_0) = 256 \times 10^{-6}$ m^3 (D Grade, Poor), and $S_g(\Omega_0) = 1024 \times 10^{-6}$ m^3 (E Grade, Very Poor), respectively, according to ISO 2631 standards, and choose speed from 60 km/h to 100 km/h with an interval as 10 km/h. Taking into account the random nature of the road input, the root mean square (RMS) values of driver head acceleration, car suspension stroke, seat suspension stroke, and dynamic tyre load are used as performance indices to compare the performance of integrated active suspension and passive suspension. The simulation will be randomly run 100 times to calculate the expectation of RMS values, and the results under three different road profiles and five different speeds are compared in Figures 10–12. It can be observed from Figures 10–12 that the integrated static output feedback Controller V always outperforms the passive suspension in terms of head acceleration with practically accepted car suspension stroke, seat suspension stroke, and dynamic tyre load despite the change of road conditions and speeds. To show the results more clearly, one sample of random responses under D Grade road disturbance with vehicle speed 100 km/h is shown in Figure 13. It can bee seen from Figure 13 that the head acceleration is really improved by integrated active suspension in comparison to passive suspension.

4.2 Validation on A Full-Car Model

Although the proposed controller is designed for a quarter-car model, it is now applied to a full-car model to further validate its effectiveness and robustness against actuator dynamics, measurement noises and parameter uncertainties. A full-car suspension model together with a seat suspension model and a driver body is shown in Figure 14, where

$m_s = 1200$ kg, $I_\theta = 2100$ kg m^2, $I_\phi = 460$ kg m^2, $l_f = 1.011$ m, $l_r = 1.803$ m, $t_f = 0.761$ m, $t_r = 0.761$ m, $s_x = 0.3$m, $s_y = 0.25$ m [7]. The driver seat and body models are same to those described in Figure 1. Furthermore, four electro-hydraulic actuators are assumed to be installed between unsprung and sprung masses, and one electro-hydraulic actuator is placed between cabin floor and seat frame. The electro-hydraulic actuator is modelled as [33]

$$\frac{V_t}{4\beta_e}\dot{P}_L = Q_L - C_{tp}P_L - A_r(\dot{x}_s - \dot{x}_u), \tag{64}$$

where P_L is the pressure drop across the piston, A_r is the piston area of the hydraulic actuator, β_e is the effective bulk modulus, V_t is the total actuator volume, C_{tp} is the coefficient of total leakage due to pressure, Q_L is the load flow. The parameter values are given as $A_r = 3.35 \times 10^{-4}$ m^2, $\frac{V_t}{4\beta_e} = 4.515 \times 10^{13}$ N/m^5, $C_{tp} = \frac{4\beta_e}{V_t}$.

In the simulation, the designed Controller V will be applied to calculate the desired control force in terms of the measured signals for each actuator, and then, the desired forces will be tracked and applied to the vehicle and seat suspension through electro-hydraulic actuators. For simplicity, a PID controller will be applied to each actuator as an inner control loop so that each actuator can track its desired force. More advanced strategies for controlling electro-hydraulic actuator can be found, for example, in [36, 37], which, however, will not be discussed in this paper.

To validate the system performance, the bump road disturbances as shown in Figure 15 will be applied to the vehicle wheels. It is seen from Figure 15 that the road disturbances, which are applied to the front and rear wheels, have same peak amplitude with a time delay of $(l_f+l_r)/v_0$. However, to excite the roll motion of the vehicle, the road disturbances to the left and right wheels are applied with different amplitude [7].

At first, we assume that the system does not have parameter uncertainties and measurement noises. When the Controller V is applied, the driver head acceleration under the bump road disturbance is shown in Figure 16. It can be seen from Figure 16 that the proposed control strategy largely reduces the driver head acceleration compared to the passive system, and therefore, achieves good ride comfort performance. The car sus-

pension stroke, seat suspension stroke, and the dynamic tyre load are compared with the passive system in Figures 17–19, respectively. It can be seen that all the strokes are within their limitations under this bump road input and their dynamic tyre loads show that the road holding performance is kept. The actuator output forces are shown in Figure 20, where seat suspension actuator provides less force compared to wheel suspension actuators.

Under the random road disturbance, the RMS values under three different road profiles and five different speeds are also calculated. For brevity, only the results under E Grade road disturbance with different speeds are shown in Figure 21. Similar conclusion can be obtained from Figure 21 that the integrated static output feedback Controller V outperforms the passive suspension in terms of head acceleration with practically accepted car suspension stroke, seat suspension stroke, and dynamic tyre load despite the change of speeds. One sample of random responses under D Grade road disturbance with vehicle speed 100 km/h is shown in Figure 22, which also confirms the effectiveness of the designed controller.

At last, parameter uncertainties to the driver body model and measurement noises on wheel vertical accelerations, which will be integrated to get wheel velocities and displacements, are added to the full-car model. The variations to driver mass, stiffnesses and damping coefficients are randomly generated within 10 % of their nominal values. Many cases have been tested, however, to save space, only one case with the driver head acceleration under the bump road disturbance is shown in Figure 23 and the noised wheel accelerations are shown in Figure 24. It can be seen from Figure 23 that the proposed control strategy reduces the driver head acceleration compared to the passive system even when there exist parameter uncertainties and measurement noises. The robustness of the designed controller is validated to be effective.

5 Conclusions

In this paper, an integrated seat and suspension has been developed and used for an integrated controller design. As some state variables are not measurement available in practice, a static output feedback controller design method is presented. Considering the limited capability of actuators, actuator saturation constraint is included in the controller design process. Numerical simulations are used to validate the performance of the designed controllers. The results show that the integrated seat and suspension control can provide the best ride comfort performance compared to the passive seat and suspension, active seat suspension control, and active car suspension control. The static output feedback control achieves compatible performance to the state feedback control with an realisable structure. Further study on robust control of the integrated model considering more complex car models, actuator dynamics, time-varying parameter and parameter uncertainties, and measurement noise, etc., will be conducted.

Acknowledgments

The authors would like to thank the anonymous reviewers for their invaluable suggestions and comments on the improvement of the paper. The support of this work by the University of Wollongong URC Small Grant is gratefully acknowledged.

References

[1] S.-B. Choi, M.-H. Nam, and B.-K. Lee. Vibration control of a MR seat damper for commercial vehicle. *Journal of Intelligent Material Systems and Structures*, 11:936–944, 2000.

[2] I. J. Tiemessen, C. T. J. Hulshof, and M. H. W. Frings-Dresen. An overview of strategies to reduce whole-body vibration exposure on drivers: A systematic review. *International Journal of Industrial Ergonomics*, 37:245–256, 2007.

[3] C.-M. Lee, A. H. Bogatchenkov, V. N. Goverdovskiy, Y. V. Shynkarenko, and A. I. Temnikov. Position control of seat suspension with minimum stiffness. *Journal of Sound and Vibration*, 292:435–442, 2006.

[4] Y. Wan and J. M. Schimmels. Improved vibration isolating seat suspension designs based on position-dependent nonlinear stiffness and damping characteristics. *Journal of Dynamic Systems, Measurement, and Control*, 125(3):330–338, 2003.

[5] S.-B. Choi and Y.-M. Han. Vibration control of electrorheological seat suspension with human-body model using sliding mode control. *Journal of Sound and Vibration*, 303:391–404, 2007.

[6] J.-D. Wu and R.-J. Chen. Application of an active controller for reducing small-amplitude vertical vibration in a vehicle seat. *Journal of Sound and Vibration*, 274:939–951, 2004.

[7] M. Bouazara, M. J. Richard, and S. Rakheja. Safety and comfort analysis of a 3–D vehicle model with optimal non–linear active seat suspension. *Journal of Terramechanics*, 43:97–118, 2006.

[8] I. Maciejewski, L. Meyer, and T. Krzyzynski. The vibration damping effectiveness of an active seat suspension system and its robustness to varying mass loading. *Journal of Sound and Vibration*, 329(19):3898–3914, 2010.

[9] Y. Zhao, L. Zhao, and H. Gao. Vibration control of seat suspension using H_∞ reliable control. *Journal of Vibration and Control*, 16(12):1859–1879, 2010.

[10] Y. Zhao, W. Sun, and H. Gao. Robust control synthesis for seat suspension systems with actuator saturation and time-varying input delay. *Journal of Sound and Vibration*, 329(21):4335–4353, 2010.

[11] W. Sun, J. Li, Y. Zhao, and H. Gao. Vibration control for active seat suspension systems via dynamic output feedback with limited frequency charateristic. *Mechatronics*, 21:250–260, 2011.

[12] D. Hrovat. Survey of advanced suspension developments and related optimal control applications. *Automatica*, 33(10):1781–1817, 1997.

[13] R. A. Williams. Automotive active suspensions. *Proceedings of the Institution of Mechanical Engineers, Part D: Journal of Automobile Engineering*, 211(6):415–444, 1997.

[14] S.-K. Chung and H.-B. Shin. High-voltage power supply for semi-active suspension system with ER-fluid damper. *IEEE Transactions on Vehicular Technology*, 53(1):206–214, 2004.

[15] E. Guglielmino, T. Sireteanu, C. W. Stammers, G. Ghita, and M. Giuclea. *Semi-active Suspension Control - Improved Vehicle Ride and Road Friendliness*. Springer, London, 2008.

[16] I. Martins, J. Esteves, G.D. Marques, and F. Pina da Silva. Permanent-magnets linear actuators applicability in automobile active suspensions. *IEEE Transactions on Vehicular Technology*, 55(1):86–94, 2006.

[17] B. L. J. Gysen, J. J. H. Paulides, J. L. G. Janssen, and E. A. Lomonova. Active electromagnetic suspension system for improved vehicle dynamics. *IEEE Transactions on Vehicular Technology*, 59(3):1156–1163, 2010.

[18] B. L. J. Gysen, T. P. J. van der Sande, J. J. H. Paulides, and E. A. Lomonova. Efficiency of a regenerative direct-drive electromagnetic active suspension. *IEEE Transactions on Vehicular Technology*, 60(4):1384–1393, 2011.

[19] J. Wang, W. Wang, and K. Atallah. A linear permanent-magnet motor for active vehicle suspension. *IEEE Transactions on Vehicular Technology*, 60(1):55–63, 2011.

[20] Z. Zhang, N. C. Cheung, K. W. E. Cheng, X. Xue, and J. Lin. Direct instantaneous force control with improved efficiency for four-quadrant operation of linear switched reluctance actuator in active suspension system. *IEEE Transactions on Vehicular Technology*, 61(4):1567–1576, 2012.

[21] O. Gundogdu. Optimal seat and suspension design for a quarter car with driver model using genetic algorithms. *International Journal of Industrial Ergonomics*, 37:327–332, 2007.

[22] A. Kuznetsov, M. Mammadov, I. Sultan, and E. Hajilarov. Optimization of a quarter-car suspension model coupled with the driver biomechanical effects. *Journal of Sound and Vibration*, 330:2937–2946, 2011.

[23] H. Du, N. Zhang, and J. Lam. Parameter-dependent input-delayed control of uncertain vehicle suspensions. *Journal of Sound and Vibration*, 317(3):537–556, 2008.

[24] J. H. Kim and F. Jabbari. Actuator saturation and control design for buildings under seismic excitation. *Journal of Engineering Mechanics*, 128(4):403–412, 2002.

[25] K. Zhou and P. P. Khargonekar. An algebraic Riccati equation approach to H_∞ optimization. *Systems & Control Letters*, 11:85–91, 1988.

[26] S. Boyd, L. El Ghaoui, E. Feron, and V. Balakrishnan. *Linear Matrix Inequalities in System and Control Theory*. SIAM, Philadelphia, PA, June 1994.

[27] Y.-Y. Cao and Z. Lin. Robust stability analysis and fuzzy-scheduling control for nonlinear systems subject to actuator saturation. *IEEE Transactions on Fuzzy Systems*, 11(1):57–67, 2003.

[28] V. L. Syrmos, C. T. Abdallah, P. Dorato, and K. Grigoriadis. Static output feedback — a survey. *Automatica*, 33(2):125–137, 1997.

[29] H. Du and N. Zhang. Designing H_∞/GH_2 static-output feedback controller for vehicle suspensions using linear matrix inequalities and genetic algorithms. *Vehicle System Dynamics*, 46(5):385–412, 2008.

[30] H. Du and N. Zhang. Static output feedback control for electrohydraulic active suspensions via TS fuzzy model approach. *Journal of Dynamic Systems, Measurement, and Control*, 131(5):1–11, 2009.

[31] D. W. C. Ho and Y. Niu. Robust fuzzy design for nonlinear uncertain stochastic systems via sliding-mode control. *IEEE Transactions on Fuzzy Systems*, 15(3):350–358, 2007.

[32] H. Gao and T. Chen. Network-based H_∞ output tracking control. *IEEE Transactions on Automatic Control*, 53(3):655–667, 2008.

[33] H. Chen and K. Guo. Constrained H_∞ control of active suspensions: an LMI approach. *IEEE Transactions on Control Systems Technology*, 13(3):412–421, 2005.

[34] I. Maciejewskia, L. Meyerb, and T. Krzyzynski. Modelling and multi-criteria optimisation of passive seat suspension vibro-isolating properties. *Journal of Sound and Vibration*, 324:520–538, 2011.

[35] G. Verros, S. Natsiavas, and C. Papadimitriou. Design optimization of quarter-car models with passive and semi-active suspensions under random road excitation. *Journal of Vibration and Control*, 11:581–606, 2005.

[36] A. Alleyne and R. Liu. Systematic control of a class of nonlinear systems with application to electrohydraulic cylinder pressure control. *IEEE Transactions on Control Systems Technology*, 8(4):623–634, 2000.

[37] A. G. Thompson and B. R. Davis. Force control in electrohydraulic active suspensions revisited. *Vehicle System Dynamics*, 35(3):217–222, 2001.

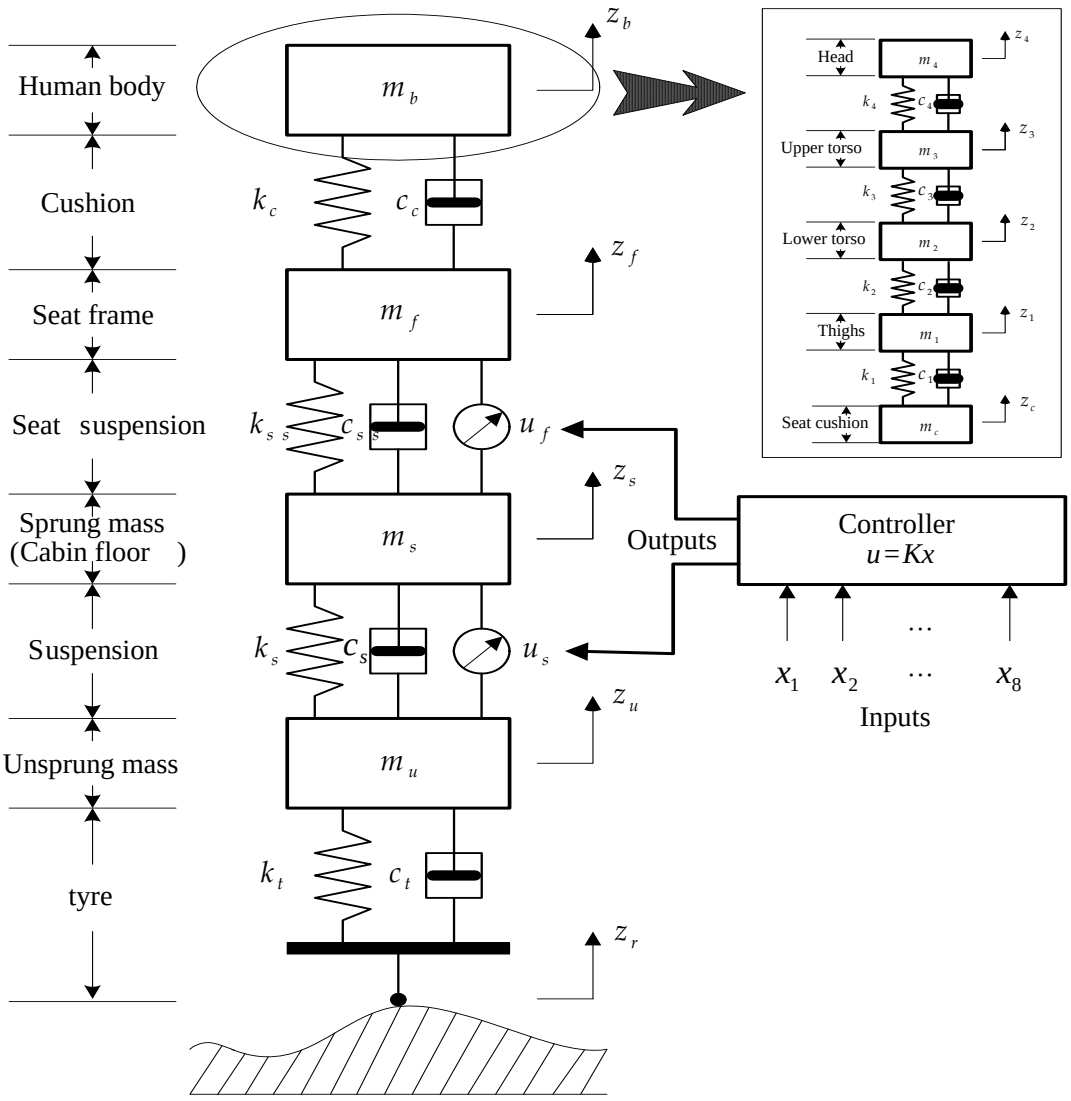

Figure 1: Integrated seat and suspension model.

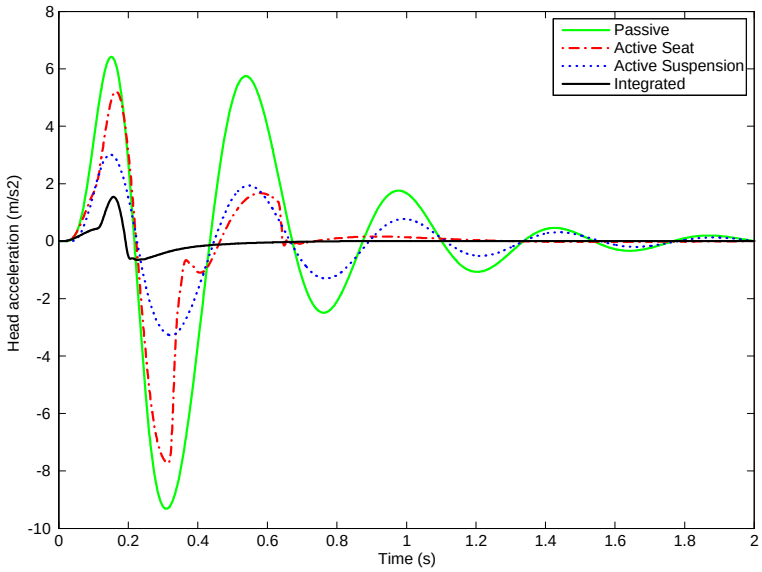

Figure 2: Bump responses on driver head acceleration for different control systems.

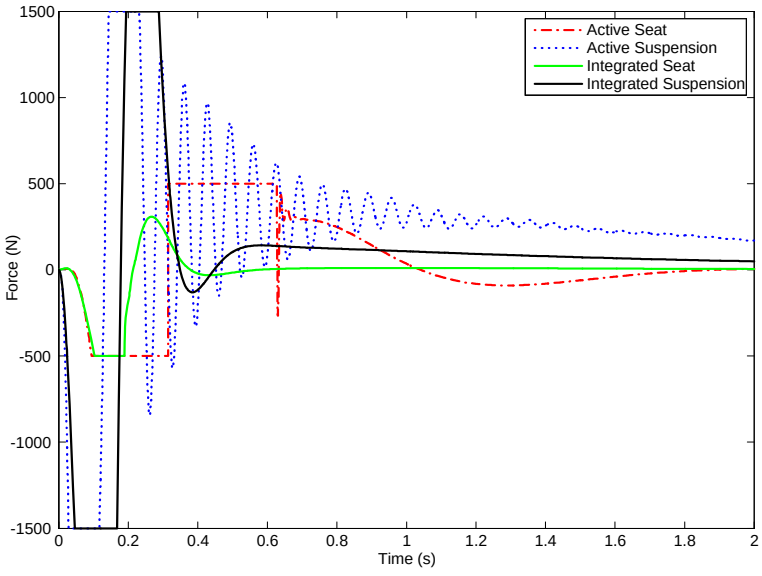

Figure 3: Control forces under bump road disturbance.

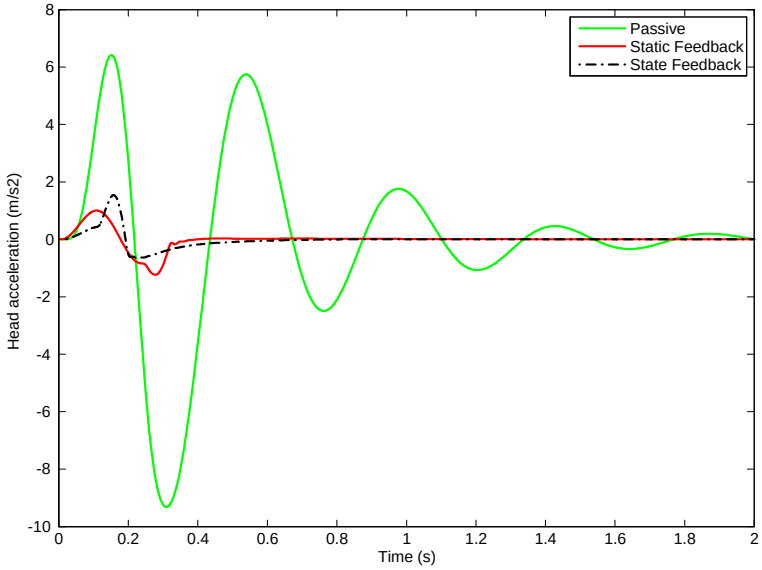

Figure 4: Bump responses on driver head acceleration for state feedback control and static output feedback control.

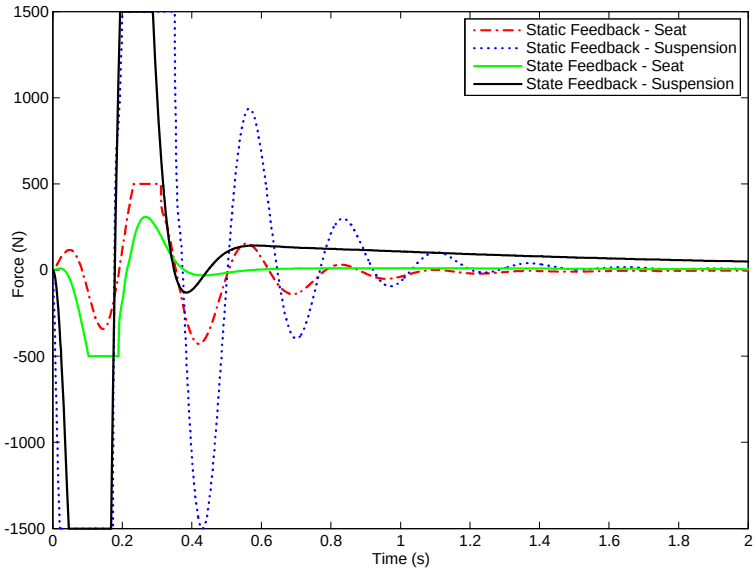

Figure 5: Control forces under bump road disturbance for state feedback control and static output feedback control.

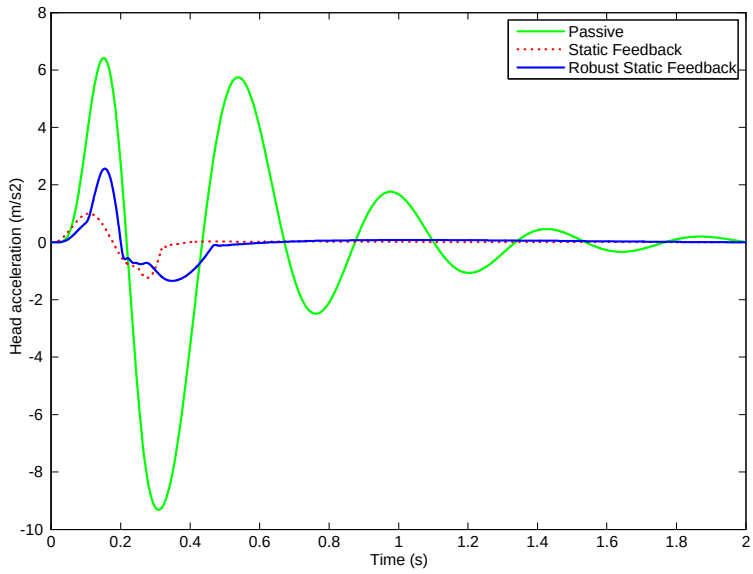

Figure 6: Bump responses on driver head acceleration for static feedback control and robust static output feedback control.

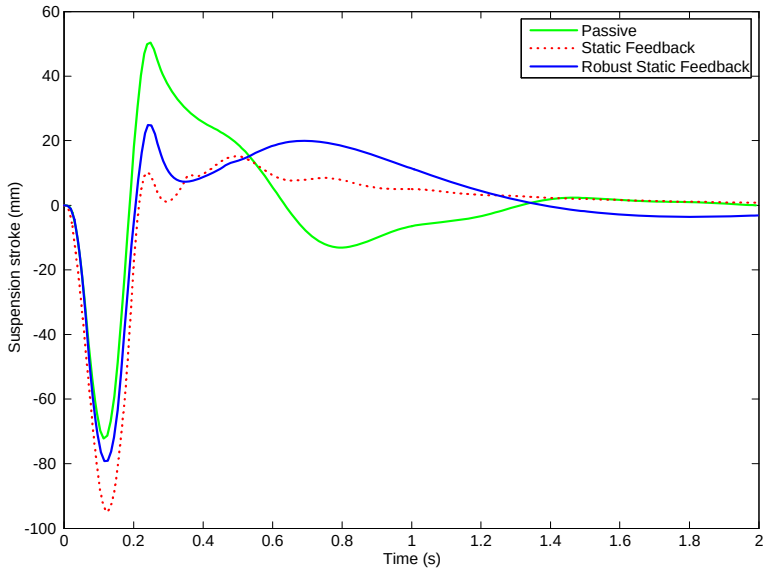

Figure 7: Bump responses on car suspension stroke for static feedback control and robust static output feedback control.

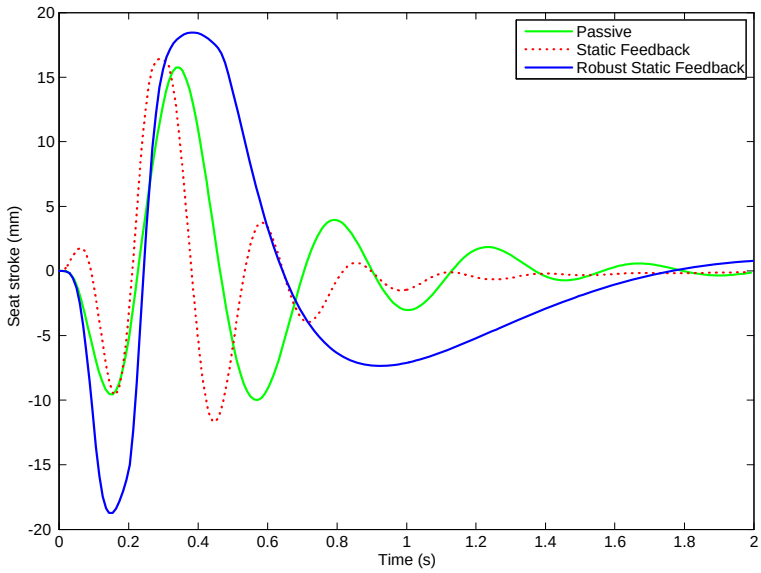

Figure 8: Bump responses on seat suspension stroke for static feedback control and robust static output feedback control.

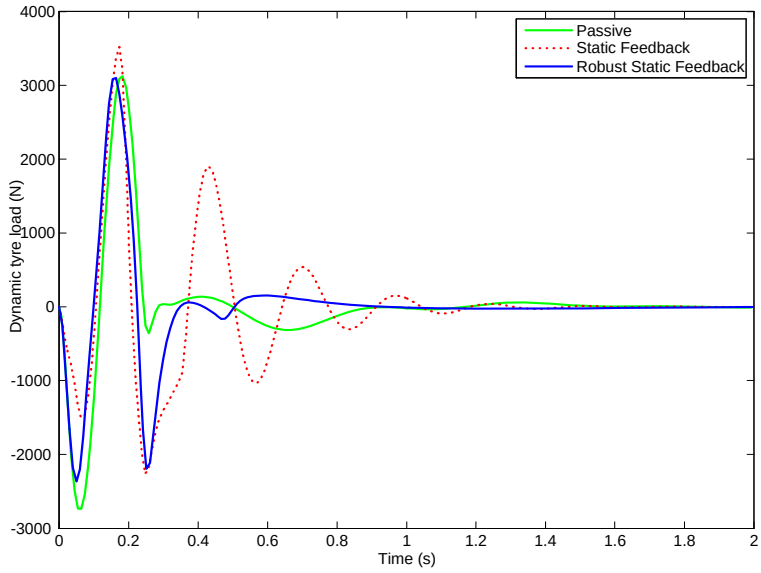

Figure 9: Bump responses on dynamic tyre load for static feedback control and robust static output feedback control.

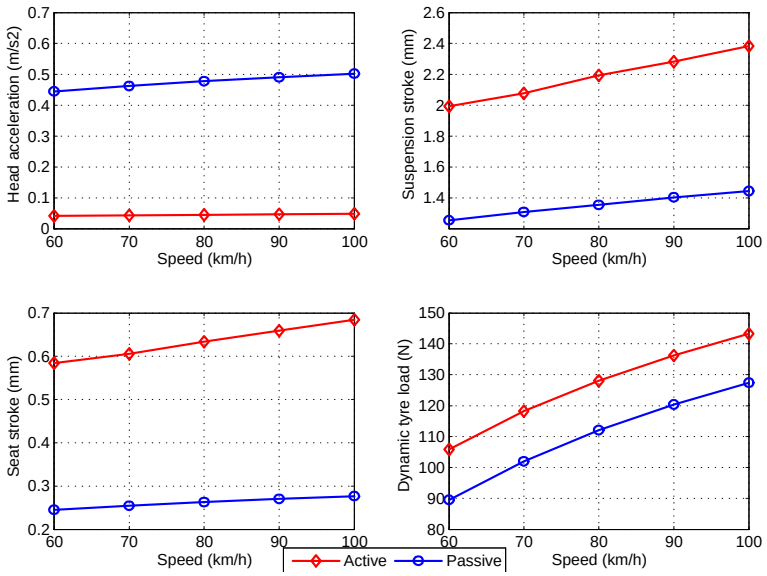

Figure 10: RMS of random responses under C Grade road disturbance with different vehicle speeds.

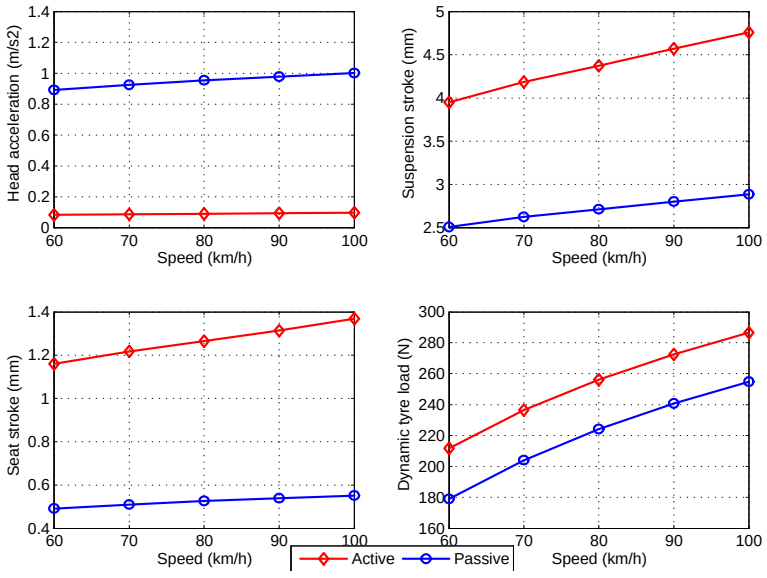

Figure 11: RMS of random responses under D Grade road disturbance with different vehicle speeds.

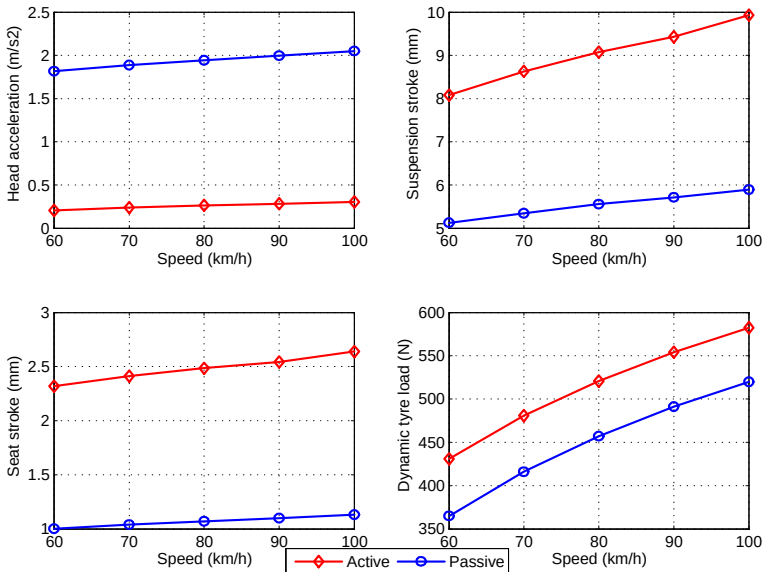

Figure 12: RMS of random responses under E Grade road disturbance with different vehicle speeds.

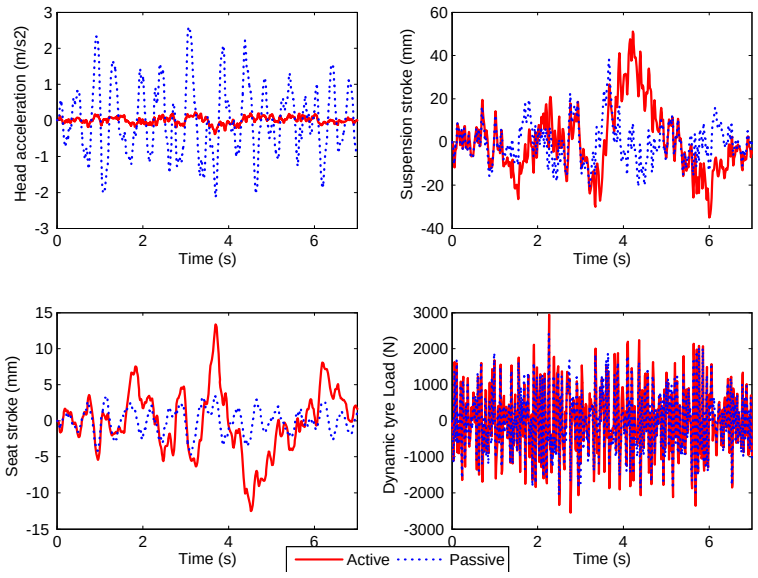

Figure 13: Random responses under D Grade road disturbance with vehicle speed of 100 km/h.

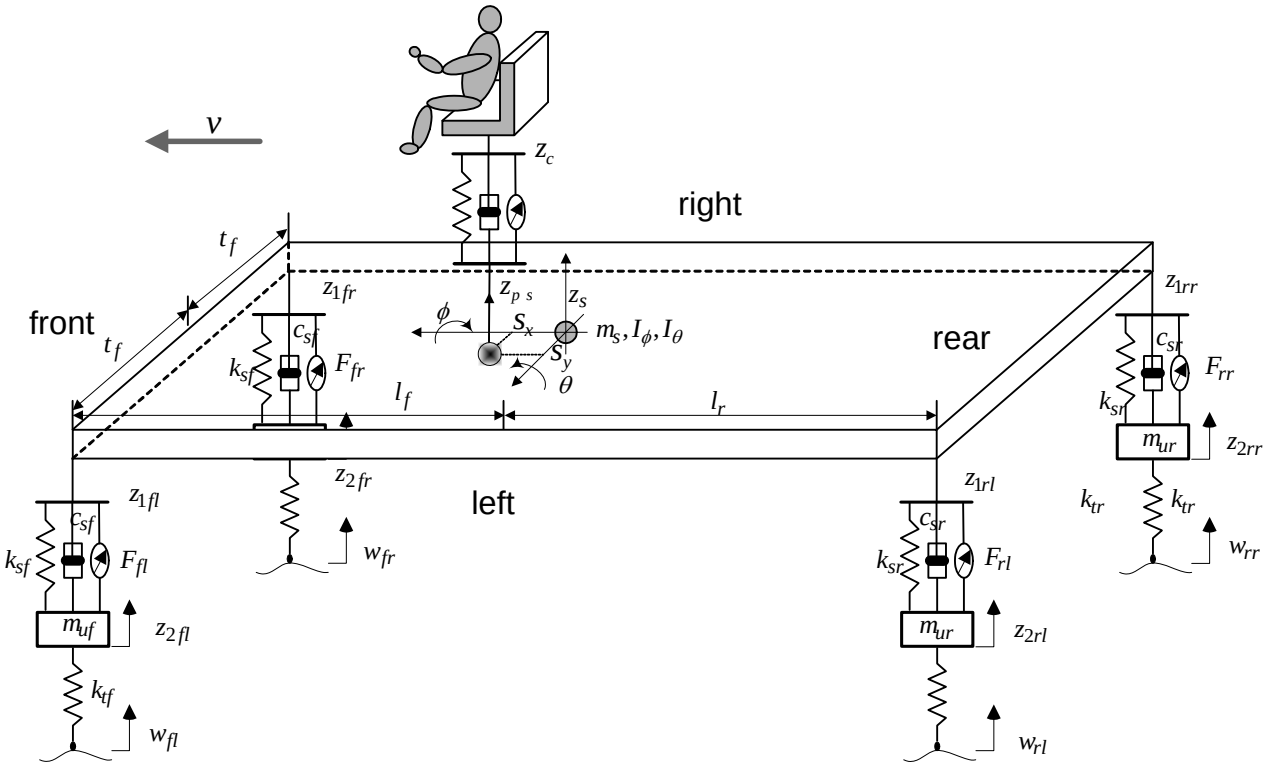

Figure 14: The full-car suspension model with a driver seat.

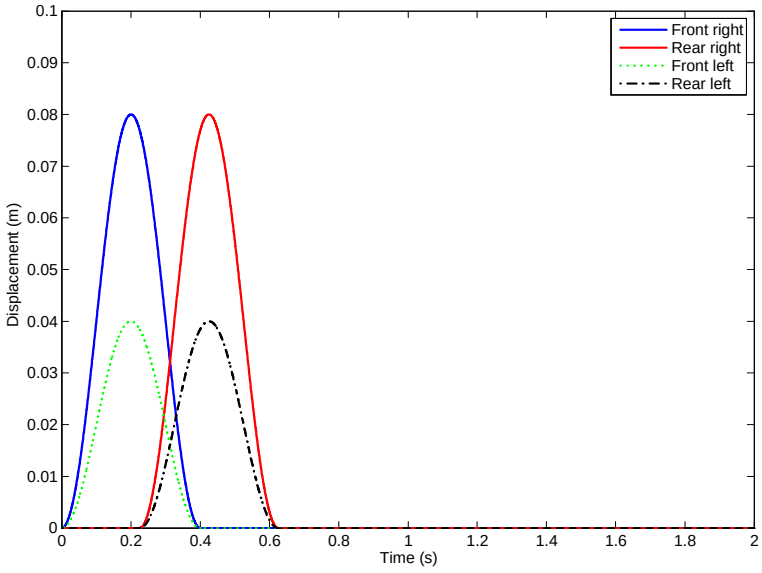

Figure 15: Road disturbance.

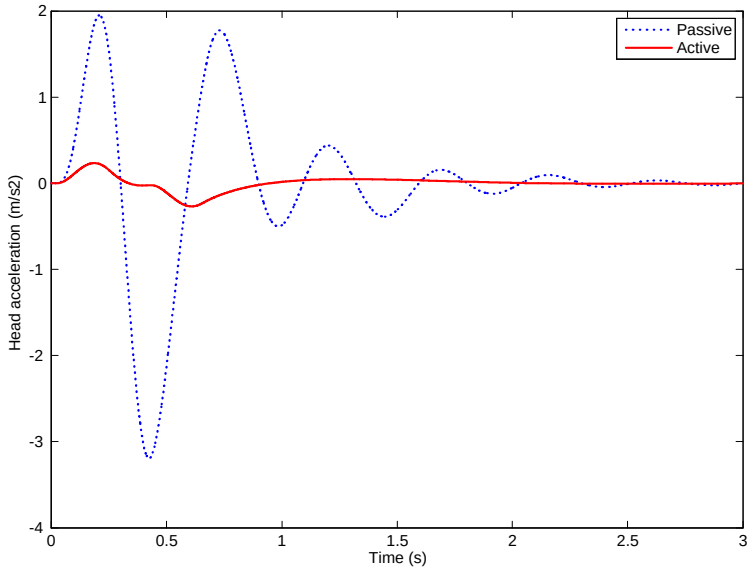

Figure 16: Bump responses on driver head acceleration for a full-car suspension without parameter uncertainties and measurement noises.

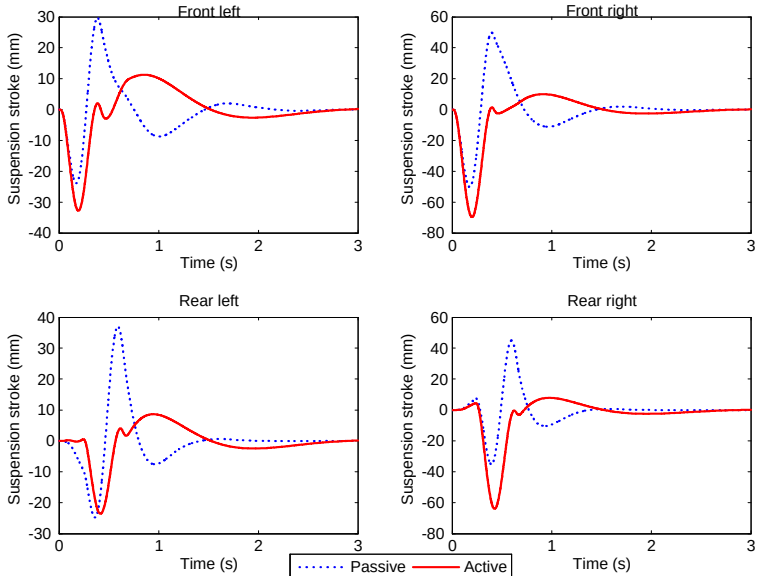

Figure 17: Car suspension strokes under bump road disturbances.

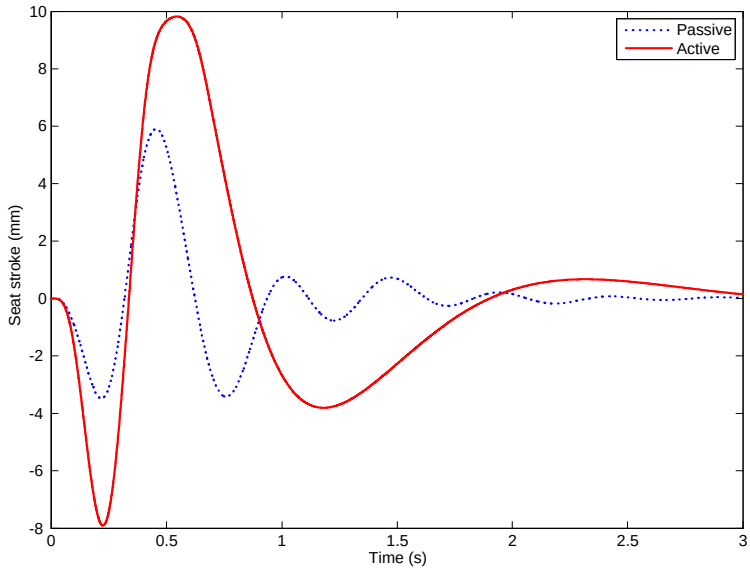

Figure 18: Seat suspension strokes under bump road disturbances.

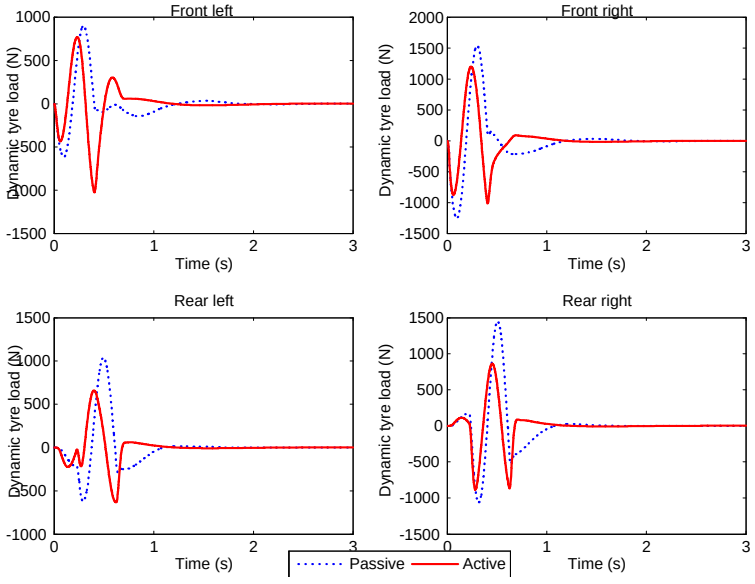

Figure 19: Dynamic tyre loads under bump road disturbances.

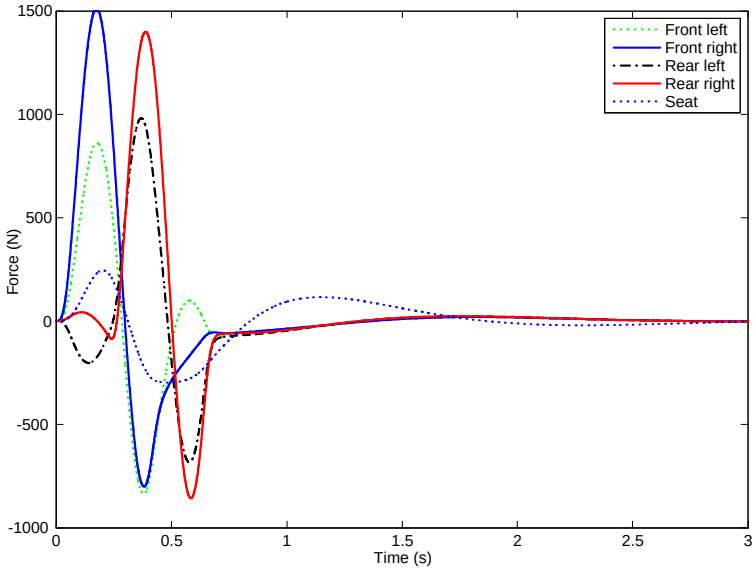

Figure 20: Actuator output forces under bump road disturbances.

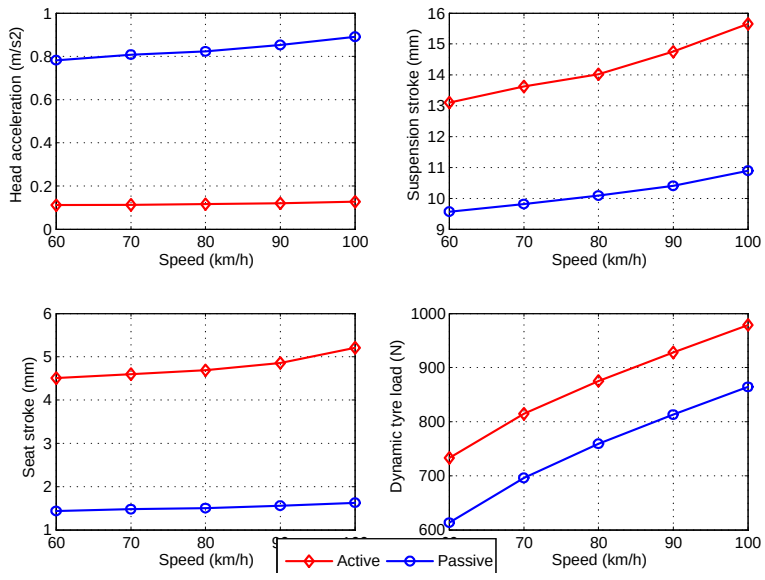

Figure 21: RMS of random responses under E Grade road disturbance with different vehicle speeds.

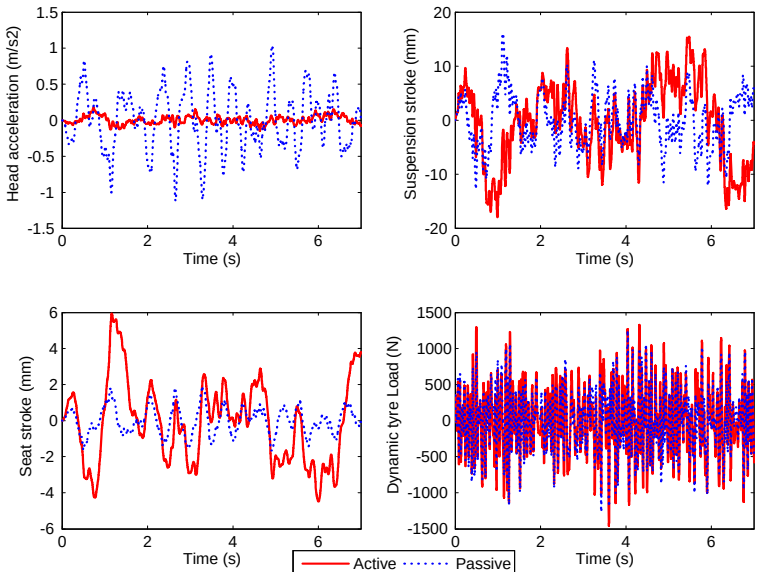

Figure 22: Random responses under D Grade road disturbance with vehicle speed of 100 km/h.

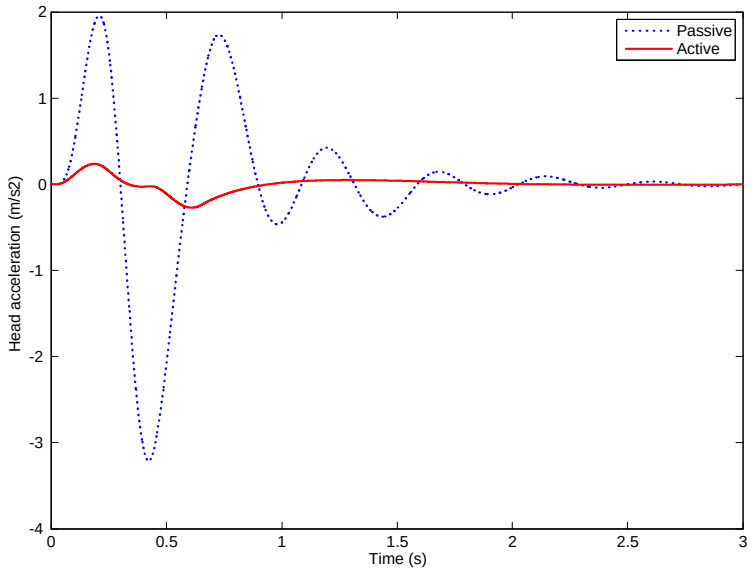

Figure 23: Bump responses on driver head acceleration for a full-car suspension with parameter uncertainties and measurement noises.

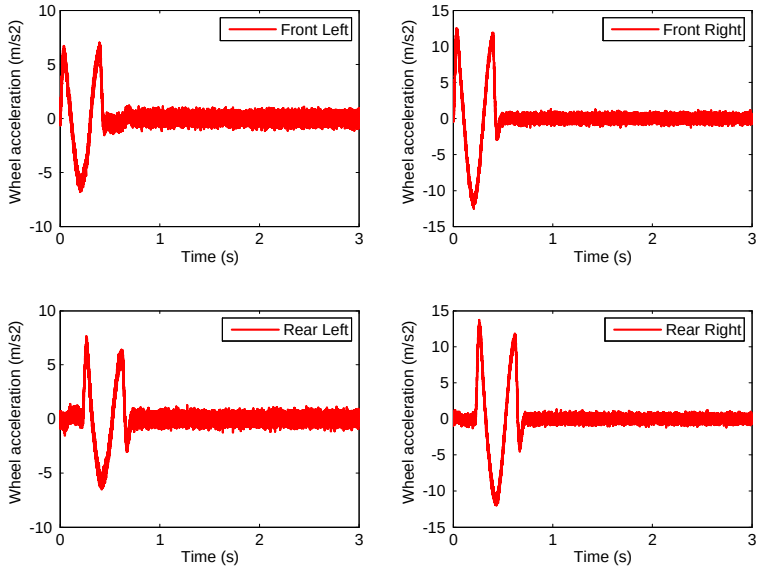

Figure 24: Wheel vertical accelerations with measurement noises.